Compact stars for undergraduates

Compact stars for undergraduates

Irina Sagert, Matthias Hempel, Carsten Greiner and Jürgen Schaffner-Bielich

Institut für Theoretische Physik, J W Goethe Universität, Max-von-Laue-Straße 1,
D-60438 Frankfurt am Main, Germany

E-mail: sagert@astro.uni-frankfurt.de, hempel@astro.uni-frankfurt.de,
carsten.greiner@th.physik.uni-frankfurt.de and schaffner@astro.uni-frankfurt.de

Abstract
We report on an undergraduate student project initiated in the summer semester
of 2004 with the aim to establish equations of state for white dwarfs and neutron
stars for computing mass–radius relations as well as corresponding maximum
masses. First, white dwarfs are described by a Fermi gas model of degenerate
electrons and neutrons, and effects from general relativity are examined. For
neutron star matter, the influence of a finite fraction of protons and electrons
and of strong nucleon–nucleon interactions are studied. The nucleon–nucleon
interactions are introduced within a Hartree–Fock scheme using a Skyrme-type
interaction. Finally, masses and radii of neutron stars are computed for a given
central pressure.

1. Introduction

Compact stars, i.e. white dwarfs and neutron stars, are the final stages in the evolution of
ordinary stars. After hydrogen and helium burning, the helium reservoir in the star's core
is burned up to carbon and oxygen. The nuclear processes in the core will stop and the
star's temperature will decrease. Consequently, the star shrinks and the pressure in the core
increases.

As long as the star's mass is above a certain value, it will be able to initialize new fusion
processes to heavier elements. The smaller the mass, the more the core has to be contracted
to produce the required heat for the next burning process to start. If the star's initial mass is
below eight solar masses, the gravitational pressure is too weak to reach the required density
and temperature to initialize carbon fusion. Due to the high core temperature, the outer regions
of the star swell and are blown away by stellar winds. What remains is a compact core mainly
composed of carbon and oxygen. The interior consists of a degenerate electron gas which, as
we will discuss, is responsible for the intrinsic high pressure. The compact remnant starts to
emit its thermal energy and a white dwarf is born.

As there are no fusion processes taking place in the interior of the white dwarf, a different force than thermal pressure is needed to keep the star in hydrostatic equilibrium. Due to the Pauli principle, two fermions cannot occupy the same quantum state; hence, more than two electrons (with different spins) cannot occupy the same phase space. With increasing density, the electrons fill up the phase space from the lowest energy state, i.e. the smallest momentum. Consequently, the remaining electrons sit in physical states with increasing momentum. The resulting large velocity leads to an adequate pressure of the electrons—the degeneracy pressure—counterbalancing gravity's pull and stabilizing the white dwarf.

The electrons are the first particles to become degenerate in dense matter due to their small mass. White dwarfs consist also of carbon and oxygen, but the contribution of nuclei to the pressure is negligible for the density region of interest here. The gravitational force increases with mass. Consequently, a larger degeneracy pressure, i.e. a greater density, is needed for stability for more massive white dwarfs. There is a mass limit for white dwarfs beyond which even the degenerate electron gas cannot prevent the star from collapsing. This mass limit is around 1.4 solar masses—the famous Chandrasekhar mass. For greater masses, the white dwarf collapses to a neutron star or a black hole. The radii of white dwarfs are in the range of 10 000 km—about the size of our planet Earth.

Similarly, a neutron star is also stabilized by the degeneracy pressure also. The difference is that for neutron stars the degeneracy pressure originates mainly from neutrons, not from electrons.

If the initial mass of an ordinary star exceeds eight solar masses, carbon and oxygen burning starts in the core. Around the core are a layer of helium and a layer of hydrogen, both taking part in fusion processes. As long as they produce the required temperature to keep the star in hydrostatic equilibrium, new burning processes to heavier elements will take place in the core while the fusion of lighter elements will continue in the outer shells. Once iron is produced in the core, there is no burning process left to generate energy as the fusion to heavier elements requires energy to be put in. So the mass of the iron core increases while its radius decreases as there is less thermal pressure to work against gravity. At some critical mass, the iron core collapses. The density increases so much that the electrons are captured by nuclei and combine with protons to form neutrons. Therefore, the atomic nuclei become more and more neutron-rich with increasing density. At some critical density, the nuclei are not able to bind all the neutrons anymore, neutrons start to drop out and form a neutron liquid which surrounds the atomic nuclei. For even larger density, there will be just a dense and incompressible core of neutrons with a small fraction of electrons and protons. Neutrons in neutron stars are then degenerate like electrons in white dwarfs.

There will be an outgoing shock wave generated by the proto-neutron star due to the high incompressibility of neutron star matter. The falling outer layers of the ordinary star bounce and move outwards interacting with the other still collapsing layers and generate an overall outward expansion—a core-collapse supernova arises. The neutron-rich remnant of the core collapse will become a neutron star as long as its mass is less than about two to three solar masses, otherwise it proceeds to shrink and finally becomes a black hole. The radii of neutron stars are typically 10 km—the size of the city of Frankfurt.

During the summer semester of 2004, the last two co-authors organized a student project about compact stars on which we will give an extended report in the following. We derive the equations of state (EoSs) for white dwarfs and neutron stars, respectively, where we will cover the Newtonian and the relativistic cases for both kinds of compact star. These EoSs are used to determine numerically the masses and radii for a given central pressure. In section 2.1, we give a short description of the properties of white dwarfs and neutron stars. We then proceed in section 2.2 with calculations of the EoS for white dwarfs. We assume a Fermi gas model

of degenerate electrons and outline two different ways which we employed for deriving the equations of state, repeat the basic structure equations for stars as well as the corrections from general relativity (the so-called Tolman–Oppenheimer–Volkoff (TOV) equation) and discuss the Chandrasekhar mass, which is the famous mass limit for white dwarfs. From section 3 onwards, we will concentrate on neutron stars. Again we will have two different approaches for calculating the equation of state for neutron stars. After describing a pure neutron star, we will discuss the effect of the presence of protons and electrons which will appear in β-equilibrium. Furthermore, we will introduce a simple effective model for incorporating the nucleon–nucleon interactions. We will compare our results to the recent work by Silbar and Reddy [1] who are using different numerical methods and another model for the nucleon–nucleon interactions. We investigate whether the two model descriptions satisfy causality. Finally, we summarize our findings and give a short outline of modern developments in neutron star physics.

2. White dwarfs

2.1. Definitions

2.1.1. Structure equations. There are two forces acting on the star, one of them is gravitation and the second one arises from the pressure (thermal pressure for normal stars and degeneracy pressure for white dwarfs and neutron stars). The pressure and the force are related in the standard way:

$$dp = \frac{dF}{A} = \frac{dF}{4\pi r^2},\tag{1}$$

where p denotes the pressure, F is the force and A is the area where the force takes effect. For the gravitational force, one has for a spherical symmetric system:

$$dF = -\frac{G\,dm \cdot m(r)}{r^2},\tag{2}$$

with r being the radial distance of a spherical star and

$$dm = \rho(r)\,dV = \rho(r)4\pi r^2\,dr.\tag{3}$$

Equating both expressions gives the first basic structure equation for stars in general:

$$\frac{dp}{dr} = -\frac{G\rho(r)m(r)}{r^2}.\tag{4}$$

Here G is Newton's gravitational constant, ρ is the mass density, m is the mass up to radius r and V is the volume. Again using equation (3), one also has the equation

$$\frac{dm}{dr} = \rho(r)4\pi r^2.\tag{5}$$

We can rewrite the mass density in terms of the energy density ϵ:

$$\rho(r) = \frac{\epsilon(r)}{c^2},\tag{6}$$

where c is the speed of light. With these definitions, one obtains structure equations which describe how the mass and the pressure of a star change with radius:

$$\frac{dm}{dr} = \frac{4\pi r^2\epsilon(r)}{c^2},\tag{7}$$

$$\frac{dp}{dr} = -\frac{G\epsilon(r)m(r)}{c^2 r^2}.\tag{8}$$

Here one has to solve two coupled differential equations. Note that while $\mathrm{d}m/\mathrm{d}r$ is positive, $\mathrm{d}p/\mathrm{d}r$ must always be negative. Starting with certain positive values for m and p in a small central region of the star, the mass will increase while the pressure decreases eventually reaching zero. One sets $m(r = 0) = 0$ and, in addition, one has to specify some 'initial' central pressure $p(r = 0) = p_0$ in order to solve for equations (7) and (8). The behaviour of m and p as a function of the radius will become important for our numerical computations.

2.1.2. Equations of state. From the previous section, we arrived at two coupled differential equations for the mass and the pressure in a star where both depend on the energy density ϵ. One needs to fix now the relation $p(\epsilon)$ between the pressure and the energy density, in addition. Matter in white dwarfs can be treated as an ideal Fermi gas of degenerate electrons. For electrically neutral matter, an adequate number of protons to the electron gas has to be added. Furthermore, the protons combine with neutrons and form nuclei which will also be taken into account.

The distribution of fermions as an ideal gas in equilibrium in dependence of their energy is described by the Fermi–Dirac statistic:

$$f(E) = \frac{1}{\exp[(E - \mu)/k_\mathrm{B}T] + 1}, \tag{9}$$

where E is the energy, μ is the chemical potential, k_B is the Boltzmann constant and T is the temperature. In kinetic theory, we find the following correlation between the distribution function f and the number density $n_i = \mathrm{d}N_i/\mathrm{d}V$ in phase space for a certain particle species i:

$$\frac{\mathrm{d}n_i}{\mathrm{d}^3k} = \frac{g}{(2\pi\hbar)^3} f, \tag{10}$$

$(2\pi\hbar)^3$ is the 'unit' volume of a cell in phase space and g is the number of states of a particle with a given value of momentum k. For electrons, g equals 2. The number density of species i is given by

$$n_i = \int \mathrm{d}n_i = \int \frac{g}{(2\pi\hbar)^3} f \, \mathrm{d}^3k. \tag{11}$$

For degenerate fermions, the temperature can be set to zero (as $(\mu - m_\mathrm{e}c^2) \gg k_\mathrm{B}T$) and accordingly $\mu/k_\mathrm{B}T$ goes to infinity. To be added to the system, a particle must have an energy equal to the Fermi energy of the system as all the other energy levels are already filled. This description exactly matches the definition of the chemical potential, and so we can set here $\mu = E_\mathrm{F}$. With all these assumptions, we can write the distribution function as

$$f(E) = \begin{cases} 1, & \text{for } E \leqslant E_\mathrm{F}, \\ 0, & \text{for } E > E_\mathrm{F}. \end{cases} \tag{12}$$

If we ignore all electrostatic interactions, we can write for the number density of the degenerate electron gas:

$$n_\mathrm{e} = \int_0^{k_\mathrm{F}} \frac{2}{(2\pi\hbar)^3} \mathrm{d}^3k = \frac{8\pi}{(2\pi\hbar)^3} \int_0^{k_\mathrm{F}} k^2 \, \mathrm{d}k = \frac{k_\mathrm{F}^3}{3\pi^2\hbar^3}. \tag{13}$$

As the star should be electrically neutral, each electron is neutralized by a proton. If we assume that the white dwarf is predominantly made of $^{12}\mathrm{C}$ or $^{16}\mathrm{O}$ then $A/Z = 2$. The proton and neutron masses are both much larger than the electron mass, so when we calculate the

mass density in the white dwarf we can neglect the mass of the electrons and just concentrate on the nucleon mass m_N. The mass density in terms of m_N is

$$\rho = n \cdot m_N \cdot \frac{A}{Z}, \tag{14}$$

where $n = n_e$. With this equation and the dependence of number density on k_F, we find

$$k_F = \hbar \left(\frac{3\pi^2 \rho}{m_N} \frac{Z}{A} \right)^{1/3}. \tag{15}$$

As the momentum of the nucleons is negligible compared to their rest mass, the nucleons do not give a significant contribution to the pressure at zero temperature. On the other hand, the electrons behave as a degenerate gas and have large velocities which give the dominant contribution to the pressure. The energy density can be divided into two components, one term coming from nucleons and the other one coming from electrons, whereas the contribution from nucleons dominates. The complete energy density can be written as [2]

$$\epsilon = n m_N \frac{A}{Z} c^2 + \epsilon_{elec}(k_F), \tag{16}$$

where $\epsilon_{elec}(k_F)$ is the energy density of electrons. With the electron energy

$$E(k) = \sqrt{k^2 c^2 + m_e^2 c^4}, \tag{17}$$

we can write ϵ_{elec} in the following way:

$$\begin{aligned}
\epsilon_{elec}(k_F) &= \frac{8\pi}{(2\pi\hbar)^3} \int_0^{k_F} E(k) k^2 \, dk \\
&= \frac{8\pi}{(2\pi\hbar)^3} \int_0^{k_F} \left(k^2 c^2 + m_e^2 c^4 \right)^{1/2} k^2 \, dk \\
&= \epsilon_0 \int_0^{k_F/m_e c} (u^2 + 1)^{1/2} u^2 \, du \\
&= \frac{\epsilon_0}{8} [(2x^3 + x)(1 + x^2)^{1/2} - \sinh^{-1}(x)],
\end{aligned} \tag{18}$$

with

$$\epsilon_0 = \frac{m_e^4 c^5}{\pi^2 \hbar^3} \tag{19}$$

and

$$x = k_F / m_e c. \tag{20}$$

The factor ϵ_0 carries the dimension of an energy density (dyne cm^{-2}). The pressure of a system with an isotropic distribution of momenta is given by

$$p = \frac{1}{3} \frac{8\pi}{(2\pi\hbar)^3} \int_0^{k_F} k v k^2 \, dk, \tag{21}$$

where the velocity $v = k c^2 / E$ and the factor $1/3$ comes from isotropy. For the electrons, we get

$$\begin{aligned}
p(k_F) &= \frac{1}{3} \frac{8\pi}{(2\pi\hbar)^3} \int_0^{k_F} \frac{k^2 c^2}{E(k)} k^2 \, dk \\
&= \frac{8\pi}{3(2\pi\hbar)^3} \int_0^{k_F} \left(k^2 c^2 + m_e^2 c^4 \right)^{-1/2} c^2 k^4 \, dk \\
&= \frac{\epsilon_0}{3} \int_0^{k_F/m_e c} (u^2 + 1)^{-1/2} u^4 \, du \\
&= \frac{\epsilon_0}{24} [(2x^3 - 3x)(1 + x^2)^{1/2} + 3\sinh^{-1}(x)].
\end{aligned} \tag{22}$$

The energy density is dominated by the mass density of nucleons while the electrons contribute to most of the pressure.

We want to arrive at an equation of the form $p = p(\epsilon)$. In the following, let us consider the two extreme cases: $x \ll 1$ and $x \gg 1$, i.e. $k_F \ll m_e c$ and $k_F \gg m_e c$, respectively. In the former case, the kinetic energy is much smaller than the rest mass of the electrons, i.e. that is the non-relativistic case. Considering the equation for the pressure for $k_F \ll m_e c$, one finds that

$$p(k_F) = \frac{\epsilon_0}{3} \int_0^{k_F/m_e c} (u^2 + 1)^{-1/2} u^4 \, du$$
$$\approx \frac{\epsilon_0}{3} \int_0^{k_F/m_e c} u^4 \, du = \frac{\epsilon_0}{15} \left(\frac{k_F}{m_e c} \right)^5 = \frac{\hbar^2}{15\pi^2 m_e} \left(\frac{3\pi^2 \rho Z}{m_N A} \right)^{5/3}. \quad (23)$$

With the assumption $\epsilon = \rho \cdot c^2$, one arrives at the following equation of state (EoS) in the non-relativistic limit:

$$p \approx K_{\text{non-rel}} \epsilon^{5/3}, \quad (24)$$

with

$$K_{\text{non-rel}} = \frac{\hbar^2}{15\pi^2 m_e} \left(\frac{3\pi^2 Z}{m_N c^2 A} \right)^{5/3}. \quad (25)$$

For the relativistic case ($k_F \gg m_e$), we arrive at

$$p(\epsilon) \approx K_{\text{rel}} \epsilon^{4/3}, \quad (26)$$

where

$$K_{\text{rel}} = \frac{\hbar c}{12\pi^2} \left(\frac{3\pi^2 Z}{m_N c^2 A} \right)^{4/3}. \quad (27)$$

The relation of the form

$$p = K \epsilon^\gamma \quad (28)$$

is called a 'polytropic' equation of state. With the two EoSs for the relativistic case and for the non-relativistic case, we are in a position to calculate the mass and the radius of a white dwarf with a given central energy density by inserting these relations into the structure equations (7) and (8). A discussion on general forms of polytropic EoSs can be found in [3].

Besides the non-relativistic and the relativistic polytropic EoS, there exists also a third case, which becomes important for later considerations—the ultra-relativistic EoS. Here one assumes for simplicity a relativistic pure electron Fermi gas with the total energy density

$$\epsilon = \epsilon_{\text{elec}}(k_F). \quad (29)$$

Just as in equation (18), one can calculate the energy density using

$$\epsilon(k_F) = \epsilon_0 \int_0^{k_F/m_e c} (u^2 + 1)^{1/2} u^2 \, du, \quad (30)$$

getting for the relativistic case

$$\epsilon = \frac{\epsilon_0}{4} x^4. \quad (31)$$

From equation (22)

$$p(k_F) = \frac{\epsilon_0}{3} \int_0^{k_F/m_e c} (u^2 + 1)^{-1/2} u^4 \, du, \quad (32)$$

one finds for $k_F \gg m_e$:

$$p = \frac{\epsilon_0}{12} x^4. \tag{33}$$

Therefore, one arrives at the general solution for an ultra-relativistic gas:

$$p = \tfrac{1}{3} \epsilon. \tag{34}$$

This relation is also very important for neutron stars as a limiting case of their relativistic EoS.

2.1.3. Chandrasekhar mass. We will derive in this section the maximum mass for white dwarfs for a polytropic EoS as found by Chandrasekhar in 1931 [4], following [2, 5]. Note that in 1932, Landau had already found with simple arguments a mass limit for white dwarfs and neutron stars [6] (see also the discussion in e.g. [2, 7]).

By straightforward algebra, the structure equations (7) and (8) can be combined to give

$$\frac{1}{r^2} \frac{d}{dr} \left(\frac{r^2}{\rho} \frac{dp}{dr} \right) = -4\pi G\rho. \tag{35}$$

The parameter γ in the polytropic equation is usually rewritten as $\gamma = 1 + \frac{1}{n}$, where n is the polytropic index.

Given the equation of state $p = p(\rho)$ in the polytropic form (see equation (28))

$$p = K\epsilon^\gamma = K\rho^\gamma c^{2\gamma}, \tag{36}$$

one can obtain $\rho(r)$ by solving equation (35) with the initial conditions:

$$\rho(r = 0) = \rho_0 \neq 0 \tag{37}$$

and

$$\left. \frac{d\rho}{dr} \right|_{(r=0)} = 0, \tag{38}$$

which follows from the condition $m(r = 0) = 0$ and equation (8). Equation (35) can be transformed into a dimensionless form with the following substitutions:

$$r = a\xi \qquad \text{with} \qquad a \equiv \left(\frac{(n+1) K \rho_0^{(1-n)/n}}{4\pi G} \right)^{1/2} c^{(n+1)/n} \tag{39}$$

and

$$\rho(r) = \rho_0 \theta^n \qquad \text{with} \qquad \theta = \theta(r). \tag{40}$$

Here θ and ξ correspond to a dimensionless density and radius, respectively, and a is a constant scale factor. With these definitions, equation (35) translates to

$$\frac{1}{\xi^2} \frac{d}{d\xi} \left(\xi^2 \frac{d\theta}{d\xi} \right) = -\theta^n. \tag{41}$$

Equation (41) is called the Lane–Emden equation for a given polytropic index n. From equation (40), one realizes that

$$\theta(r = 0) = 1. \tag{42}$$

Furthermore, with equation (38) the density distribution at the centre of the star obeys

$$\left. \frac{d\theta}{dr} \right|_{(r=0)} = 0. \tag{43}$$

With the boundary conditions, equations (43) and (42), one can integrate equation (41) numerically. One finds for $n < 5$ and $\gamma > 6/5$, respectively, that the solutions decrease

monotonically with radius and have a zero for $\xi = \xi_1$, i.e. $\theta(\xi_1) = 0$ or $\rho(r_1 = a\xi_1) = 0$, respectively. Hence, the radius of the star is given by $R = r_1 = a\xi_1$, which translates to

$$R = \left(\frac{(n+1)K\rho_0^{(1-n)/n}}{4\pi G} \right)^{1/2} c^{(n+1)/n}\xi_1. \tag{44}$$

Using equations (40) and (39), the total mass M of the star can be calculated as follows:

$$
\begin{aligned}
M &= \int_0^R 4\pi r^2 \rho \, \mathrm{d}r \\
&= 4\pi a^3 \rho_0 \int_0^{\xi_1} \xi^2 \theta^n \, \mathrm{d}\xi \\
&= 4\pi c^{(3n+3)/n} \left(\frac{(n+1)K}{4\pi G} \right)^{3/2} \rho_0^{(3-n)/2n} \xi_1^2 |\theta'(\xi_1)|.
\end{aligned}
\tag{45}
$$

For ρ_0 we can use equation (44) and get

$$M = 4\pi c^{(2n+2)/(n-1)} \left(\frac{(n+1)K}{4\pi G} \right)^{n/(n-1)} \xi_1^{(n-3)/(1-n)} \xi_1^2 |\theta'(\xi_1)| R^{(3-n)/(1-n)}. \tag{46}$$

The interesting case is the high-density limit, i.e. the relativistic case with $\gamma = \frac{4}{3}$. For this case, it follows [5] that

$$\gamma = \tfrac{4}{3}: \qquad n = 3, \qquad \xi_1 = 6.896\,85, \qquad \xi_1^2|\theta'(\xi_1)| = 2.018\,24. \tag{47}$$

For K we take equation (27) and set $\eta = A/Z$. Using these values in equation (46), we get the following expressions for the mass and the radius in the relativistic case (see [5]). For the radius,

$$R = \frac{1}{2}(3\pi)^{1/2}(6.896\,85) \left(\frac{\hbar^{3/2}}{c^{1/2}G^{1/2}m_\mathrm{e}m_\mathrm{N}\eta} \right) \left(\frac{\rho_\mathrm{crit}}{\rho_0} \right)^{1/3}, \tag{48}$$

with

$$\rho_\mathrm{crit} = \frac{m_\mathrm{N}\eta m_\mathrm{e}^3 c^3}{3\pi^2\hbar^3}, \tag{49}$$

and for the mass

$$M = \frac{1}{2}(3\pi)^{1/2}(2.018\,24) \left(\frac{\hbar c}{G} \right)^{3/2} \left(\frac{1}{m_\mathrm{N}\eta} \right)^2, \tag{50}$$

which becomes after plugging in all the values [8]

$$M = 1.4312 \left(\frac{2}{\eta} \right)^2 M_\odot. \tag{51}$$

Here and for the later calculations, we choose for m_N the neutron mass. For a white dwarf which consists mainly of ^{12}C, it is better to take the atomic mass unit (again from [8]), which gives a maximum mass of 1.4559 solar masses. It is remarkable that in the relativistic case the mass does not depend on the radius R or the central density ρ_0 anymore. As the density in the white dwarf increases, the electrons become more relativistic and the mass approaches the value of equation (51) which is the famous *Chandrasekhar* mass M_ch. It represents the maximum possible mass for a white dwarf for a purely relativistic polytropic EoS.

2.1.4. General relativity corrections. If the stars are very compact, one has to take into account effects from general relativity, like the curvature of spacetime. These effects become important when the factor $2GM/c^2R$ approaches unity. We then have to describe a compact star by using Einstein's equation

$$G_{\mu\nu} = -\frac{8\pi G}{c^4} T_{\mu\nu}. \tag{52}$$

For an isotropic, general relativistic, static, ideal fluid sphere in hydrostatic equilibrium, one arrives at the Tolman–Oppenheimer–Volkoff (TOV) equation (see e.g. [2, 5, 9, 10] for a detailed derivation)

$$\frac{\mathrm{d}p}{\mathrm{d}r} = -\frac{G\epsilon(r)m(r)}{c^2 r^2} \left[1 + \frac{p(r)}{\epsilon(r)}\right] \left[1 + \frac{4\pi r^3 p(r)}{m(r)c^2}\right] \left[1 - \frac{2Gm(r)}{c^2 r}\right]^{-1}. \tag{53}$$

This equation is similar to the differential equation for the pressure, equation (8), but has three correction factors. All three correction factors are larger than 1, i.e. they strengthen the term from Newtonian gravity. The TOV equation also contains the factor $2GM/c^2R$ which determines whether one has to take into account general relativity or not. The corresponding critical radius

$$R = \frac{2GM}{c^2} \tag{54}$$

is the so-called Schwarzschild radius. For a star with a mass of $1M_\odot$, we get $R \approx 3$ km. Hence, effects from general relativity will become quite important for neutron stars as they have radii around 10 km. The corrections are smaller for white dwarfs with radii of $R\,(M = 1M_\odot) \approx 10^4$–$10^3$ km but will be checked numerically later. For completeness, note that an anisotropy in the pressure can generate an additional term to the TOV equations even for spherical symmetry [11] which we, however, do not consider in the following.

2.2. Calculations

2.2.1. Principle. In the following, we use the structure equations (8) and (7) for our numerical calculations of the mass and the radius of white dwarfs and neutron stars. We need two initial values for the calculation, $p(0)$ and $m(0)$. From equation (5), it is clear that $m(0) = 0$. We will increase r in small steps and for each step in the radius the new pressure and new mass are calculated via

$$p(r + \Delta r) = -\frac{G\epsilon(r)m(r)}{c^2 r^2} \Delta r + p(r), \tag{55}$$

$$m(r + \Delta r) = \frac{4\pi r^2 \epsilon(r)}{c^2} \Delta r + m(r), \tag{56}$$

with Δr as a fixed constant which determines the accuracy of the calculation. This is the so-called Newton method, whereas later we also employed a four-step Runge–Kutta method which allows a more sophisticated numerical integration. As mentioned before in section 2.1.1, the pressure will decrease with increasing r. At a certain point, the pressure $p(R)$ will become zero (or even negative) which will terminate the integration and determine the radius of the star R and as its mass $M = m(R)$. For our computation, we worked with Fortran and Matlab.
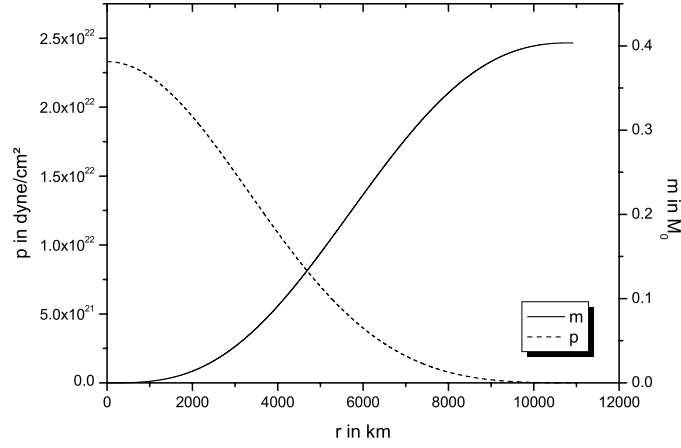
Figure 1. The mass $m(r)$ and the pressure $p(r)$ for a non-relativistic white dwarf with a central pressure of $p_0 = 2.2 \times 10^{22}$ dyne cm^{-2}.

2.2.2. Polytropic EoS. First, we will use the polytropic equation of state

$$p = K\epsilon^{\gamma}. \tag{57}$$

In this subsection, we closely follow [1]. We will just briefly discuss the method which was used in [1] as well as our results and refer the reader to the original paper for more detailed information. The complication in solving the differential equations (8) and (7) is to find a way to compute for a certain pressure $p(r)$ the corresponding energy density $\epsilon(r)$. The polytropic form of the EoS, equation (57), avoids this problem and being plugged in equation (8) gives

$$\frac{\mathrm{d}p(r)}{\mathrm{d}r} = -\frac{R_0 p(r)^{1/\gamma} \bar{m}(r)}{r^2 K^{1/\gamma}}, \tag{58}$$

with

$$\bar{m}(r) = \frac{m(r)}{M_{\odot}}, \qquad R_0 = \frac{GM_{\odot}}{c^2}, \tag{59}$$

where $M_{\odot}$ is the mass of the Sun, hence $\bar{m}(r)$ is dimensionless, and R_0 is half of the Schwarzschild radius and is given in km. We also get a new expression for the differential equation for the dimensionless mass:

$$\frac{\mathrm{d}\bar{m}(r)}{\mathrm{d}r} = \frac{4\pi r^2}{M_{\odot} c^2} \left(\frac{p(r)}{K} \right)^{1/\gamma}. \tag{60}$$

The units for energy density $\epsilon(r)$ and the pressure $p(r)$ are dyne cm^{-2}, the mass is expressed in $M_{\odot}$ and the radius in km. We can now calculate the mass and the radius of a white dwarf for a given central pressure.

We will distinguish between the relativistic case and the non-relativistic case by setting $\gamma = 4/3$ and $\gamma = 5/3$, respectively. Choosing for the central pressure $p_0 = 2.330\,02 \times 10^{22}$ dyne cm^{-2}, where this value satisfies the condition $k_{\mathrm{F}} \ll m_{\mathrm{e}}c$ (cf equation (22)), our numerical calculation with the Newtonian code gives us the curve shown in figure 1 for the pressure–radius and the mass–radius relations. The white dwarf's mass is $M = 0.403\,62 M_{\odot}$ and the radius is $R = 10\,919$ km.
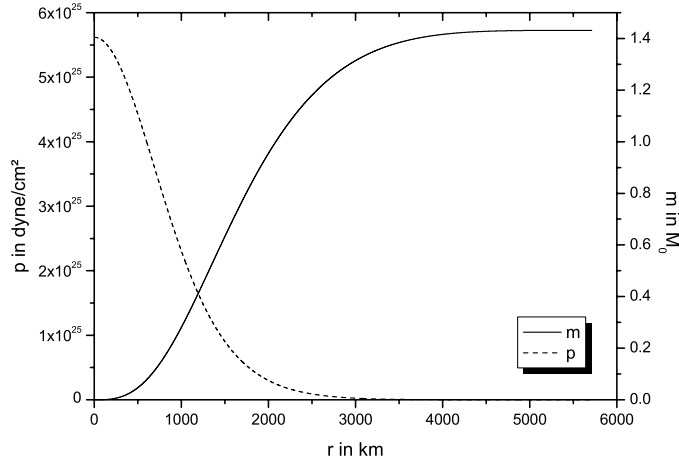
Figure 2. The mass $m(r)$ and the pressure $p(r)$ for a relativistic white dwarf with a central pressure of $p_0 = 5.62 \times 10^{25}$ dyne cm^{-2}.

To satisfy the condition $k_F \gg m_e c$ for a relativistic white dwarf, we have to choose a larger central density compared to the non-relativistic case, $p_0 = 5.619 \times 10^{25}$ dyne cm^{-2} is an appropriate value (see figure 2).

There is one interesting point as far as the relativistic polytrope is concerned. As we have seen in section 2.1.3, the mass limit to a white dwarf must be $1.4312 M_\odot$ if we set η equal to 2 and use a relativistic polytropic form for our equation of state. As these are exactly the same underlying assumptions as in our numerical computation, the maximum calculated mass must necessarily be the Chandrasekhar mass. Indeed, our numerical calculation gives us a white dwarf with a radius of 5710 km and a mass of $1.431\,45 M_\odot$. With the chosen high initial pressure value, we hit the Chandrasekhar mass limit very well.

Note, however, that according to expression (51) the mass does not depend on the central pressure. To see this in more detail, we have employed different central pressures: figure 4 shows the calculated masses of white dwarfs for initial pressures from 1×10^{23} dyne cm^{-2} to 2.5×10^{24} dyne cm^{-2}. For this range of central pressures, we always compute the same mass of $1.431\,45 M_\odot$. Hence, the numerical calculations agree with theory. As an additional check, we also plot the corresponding radii which we computed numerically (points referred to as 'R') and calculated analytically with equation (48) (referred to as 'R_{FIT}'). The deviations of the numerically computed radii from the analytical ones are about 0.2%. Taking a look at the plot, we find that for increasing central pressure the mass of the relativistic white dwarf stays constant while the corresponding radius decreases. The behaviour of the mass and the radius of a non-relativistic white dwarf with smaller central pressures is shown in figure 3 for comparison. In contrast to the relativistic case, the mass increases now with increasing central pressures.

Silbar and Reddy already pointed out in [1] that the two polytropic white dwarf models examined here are not quite physical, as the non-relativistic EoS just works for central pressures below a certain threshold while the relativistic EoS is not applicable for a small pressure. They suggest finding an EoS which covers the whole range of pressures by describing the energy density as a combination of a relativistic and a non-relativistic polytrope. We decided to try another way. On the other hand, we will employ not a guessed combination but a consistent relation $p(\epsilon)$.
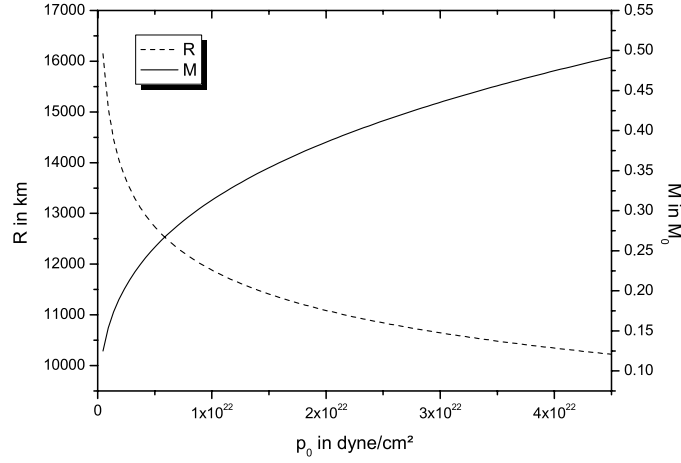
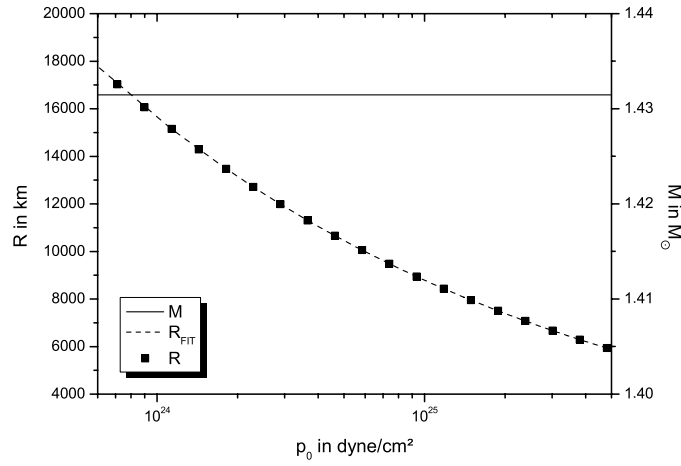**Figure 3.** Calculated masses and radii for white dwarfs using the non-relativistic polytrope.

Figure 4. Calculated masses and radii for white dwarfs using the relativistic polytropic EoS.

2.2.3. Looking for zero points. We remind the reader that it is our goal to find a relation between the energy density and the pressure which is needed for the calculation of the mass and the radius of the star. In the following, we want to use the full equations for a degenerate electron gas to derive the EoS consistently for the whole pressure range considered for white dwarfs. As we see from equations (18) and (22), it is impossible to write explicitly the energy density as a function of the pressure without using certain approximations on ϵ or p just as it was done in the previous section (i.e. the polytropic approximation).

On the other hand, a numerical solution to this problem is straightforward. As both the pressure and the energy density are functions of the Fermi momentum, we just have to find for a given pressure the corresponding Fermi momentum and use it in the equation for the energy density. With this procedure, we are able to calculate the energy density ϵ for a given pressure p. To get the Fermi momentum, we apply a root-finding method for the equation

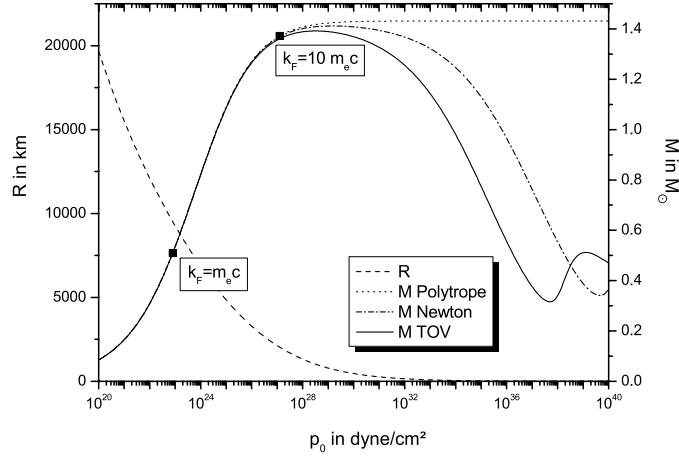$$p(k_F) - p = 0, \tag{61}$$

Figure 5. Calculated masses and radii for white dwarfs using a consistent EoS.

where p is given and $p(k_F)$ is taken from equation (22). As long as we have a simple expression for the derivative of pressure, we use the Newton–Raphson method. In other cases, when we have more complicated equations of state, we take a simple bisection method, which is less accurate, but easier to handle. In addition, we write the energy density as the sum of the nucleon energy density and the electron energy density (in the polytropic approximation the energy density of the electrons was ignored). Employing this numerical prescription to the solution for the EoS, we can calculate the mass/pressure and the radius/pressure dependences, just as in the polytrope case.

In section 2.1.4, we discussed the corrections from general relativity and we will now test their influence on the masses and radii of white dwarfs. Figure 5 shows our calculations for three different cases. In the case referred to as 'polytrope', the energy density is given just by the nucleons, as in the polytropic EoS earlier. The 'Newton' mass/pressure curve is calculated with an energy density consisting of both the nucleon and the electron energy density (see equation (16)); for the 'TOV' curve, the EoS is like that for 'Newton' but with corrections from general relativity (equation (53)). All three curves confirm the Chandrasekhar mass limit.

For pressures smaller than 10^{27} dyne cm^{-2}, the three cases are indistinguishable, while for larger pressures the curves start to deviate significantly from each other. We have indicated two points on the mass/pressure curves: the first one corresponds to a central pressure where $k_F = m_e c$, i.e. the point where the electrons start to become relativistic; the second point is at $k_F = 10 m_e c$ and marks a central pressure where the electrons are highly relativistic. At the latter point, one can already see how the three curves start to deviate from each other. The similar behaviour for low pressure is due to the fact that the electron contribution to the energy density as well as the corrections from general relativity is negligible. This is the non-relativistic region and the behaviour of the curves is comparable to that of the non-relativistic polytrope ($p \propto \epsilon^{5/3}$), the mass increases with the central pressure.

The difference of the three curves in figure 5 starts to appear around $p_0 = 10^{27}$ dyne cm^{-2}, where $k_F = 10 m_e c$. Nevertheless, in all three cases the masses stay almost constant at a value of about $1.4 M_\odot$ around $p_0 = 10^{28}$ dyne cm^{-2}. At this pressure, the relativistic electrons dominate the mass/pressure relation as in the relativistic polytrope case ($p \propto \epsilon^{4/3}$).

We will discuss the behaviour at a greater pressure starting with the case 'polytrope'. As the energy density for this model stems solely from the nucleons, the results for the mass and
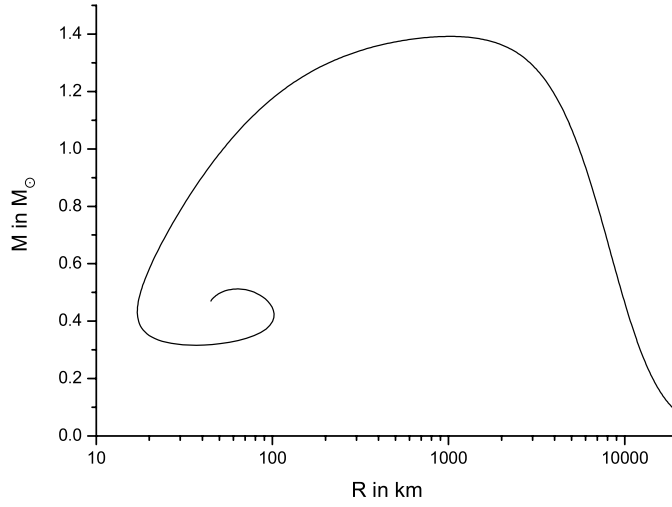
Figure 6. The mass–radius relation for white dwarfs with corrections for general relativity.

the radius for higher pressures have to merge into those of the relativistic polytrope. This is confirmed by the constant mass of 1.4314 solar masses (equal to the Chandrasekhar mass) for central densities above $p_0 = 10^{31}$ dyne cm^{-2}. The mass in the centre of the white dwarfs increases with larger central densities while the radius decreases, such that the total mass stays constant.

For high pressures, the contribution of the relativistic electrons to the energy density becomes important, which is taken into account in the 'Newton' case. The EoS for electrons can only be approximated by an ultra-relativistic polytrope (see equation (34)):

$$p = \tfrac{1}{3}\epsilon. \tag{62}$$

With increasing central pressure, the range of the radius of the white dwarf where the electrons obey the ultra-relativistic limit enlarges. The deviation from the 'polytrope' curve is an effect of the growing fraction of ultra-relativistic electrons. The masses for high pressures are now smaller than those in the 'polytrope' case for the following reason: the degeneracy pressure of electrons for the same energy density will be lower in the ultra-relativistic polytrope compared to the 'polytrope' case due to an additional contribution from electrons to the energy density. Hence, the star will support less mass and the mass decreases as a function of pressure beyond the maximum mass. For the 'TOV' mass/pressure curve, we take the former case adding effects from general relativity (see equation (53)). At a pressure of $p_0 \sim 10^{28}$ dyne cm^{-2}, the mass curve of white dwarfs exhibits a clear maximum with the maximum mass being a little bit lower than that for the Newtonian cases, i.e. $M_{\max} = 1.39 M_{\odot}$. The slightly reduced maximum mass is in accord with the fact that the corrections from general relativity strengthen the gravitational force. With increasing central pressures and smaller radii, corrections become larger. Therefore, the mass of the white dwarf decreases with increasing central pressures up to a pressure of about $p_0 = 2 \times 10^{37}$ dyne cm^{-2}, here the mass starts to rise to a maximum value of about 0.51 solar masses and then decreases again. The general relativistic corrections applied in the 'TOV' curve enhance the gravitational force, so that less mass is needed to create the given central pressure.

Figure 6 shows the calculated masses for the 'TOV' case in dependence of the radius. The central pressure increases along the curve starting from the right to the left in the plot.
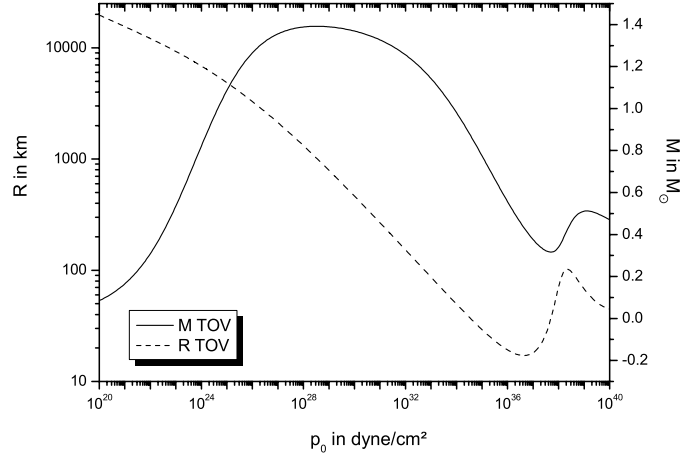
Figure 7. Calculated masses and radii for white dwarfs with corrections for general relativity.

The curve begins at large radii and small masses and continues to smaller radii and larger masses. Passing the maximum mass, the curve starts to decrease with radius. For higher central pressures, the curve starts to curl. This behaviour is typical for large central pressures, seen also in many other mass–radius relations for different equations of state. A detailed analysis of this curled shape can be found in [12, 13].

In the next subsection, we will discuss that white dwarfs of the 'Newton' and 'TOV' cases which are beyond the maximum mass limit (i.e. for $p \gg p_0$) are unstable. It can be shown that polytropic equations of state with an exponent less than 4/3 cause an instability (see e.g. [2]): an increase in energy density causes an insufficient increase in pressure to stabilize the star.

2.2.4. Stability. First, we argue that white dwarfs are unstable if $\mathrm{d}M/\mathrm{d}p_0 < 0$, following [14]. For our argumentation, we employ the mass curve in figure 7 and reason at first why white dwarfs with $p_0 \leqslant p_0^{\mathrm{max}} = p_0 \, (M = M_{\mathrm{max}})$ are stable.

Let us assume that a white dwarf oscillates radially and therefore increases its central pressure to $p_0' = p_0 + \delta p_0$ with $\delta p_0 > 0$. In figure 7, the mass curve shows white dwarfs in hydrostatic equilibrium, i.e. the degeneracy pressure and the gravitational force compensate each other. If for $p_0 \leqslant p_0^{\mathrm{max}}$ the central pressure is increased, the white dwarfs are only in hydrostatic equilibrium if their masses are larger than before. Since this is not the case, the surplus in degeneracy pressure over the gravitational attraction will expand the star back to its former state. For pressures $p_0' = p_0 - \delta p_0$, figure 7 shows that the mass $M(p_0')$ of a white dwarf in hydrostatic equilibrium is smaller than $M(p_0)$. That means that if the star expands due to radial oscillations the resulting lower central pressure can only be maintained if the gravitational force, i.e. the mass, decreases. As the mass of the white dwarf does not change, the star has to shrink again to its former state. Therefore, white dwarfs with $p_0 \leqslant p_0^{\mathrm{max}}$ and $\mathrm{d}M/\mathrm{d}p_0 > 0$ are stable.

Now we discuss the situation for a white dwarf with $p_0 > p_0^{\mathrm{max}}$ and $\mathrm{d}M/\mathrm{d}p_0 < 0$. If the central pressure is lowered to $p_0' = p_0 - \delta p_0$, then $M(p_0')$ should be larger than $M(p_0)$ to bring the star into hydrostatic equilibrium (see figure 7). So the gravitational force is not large enough to stop the expansion and the white dwarf is unstable to radial oscillations. For

an increased central pressure $p_0' = p_0 + \delta p_0$, the mass curve shows that stability is only given for a white dwarf with $p_0 \leqslant p_0^{\max}$. As the mass of the white dwarf is larger than that required for hydrostatic equilibrium, gravitation will cause the white dwarf to shrink and finally to collapse.

In [9, 13] as well as in [2], which we will follow now, a more formal approach is presented. Again, one considers radial oscillations of the white dwarf. The radial modes ω_n can be derived by solving a Sturm–Liouville eigenvalue equation with the eigenvalues ω_n^2. In doing so, one gets a range of eigenvalues with

$$\omega_0^2 < \omega_1^2 < \omega_2^2 < \cdots, \tag{63}$$

where ω_n are the eigenfrequencies to the radial modes and ω_0 corresponds to the fundamental radial mode. For the instability analysis, the so-called 'Lagrangian displacement' $\boldsymbol{\xi}(\mathbf{x}, t)$ is introduced in [2] which connects fluid elements in the unperturbed state to corresponding elements in the perturbed state. The normal modes of an oscillation can then be written as

$$\xi^i(\mathbf{x}, t) = \xi^i(\mathbf{x}) \, e^{i\omega t}, \tag{64}$$

where ξ^i are any Lagrangian displacements. Hence, the star will be stable for $\omega^2 \geqslant 0$ and unstable for $\omega^2 < 0$. This means that for stability, all modes need to have real eigenfrequencies. But because of (63) the stability of the star depends only on the sign of ω_0^2.

The instability condition can be connected to the total mass of any single star in hydrostatic equilibrium (i.e. every star lying on our $M(R)$ curve). The variation δM of the mass out of the state of equilibrium can be expressed as follows:

$$M = M_0 + \delta M + \delta^2 M, \tag{65}$$

where M_0 is the total mass at equilibrium. For all stars in hydrostatic equilibrium, it holds that the variation $\delta M = 0$. It can be shown (see [2]) that stability is given for $\delta^2 M > 0$ with an onset of instability at $\delta^2 M = 0$. For $\delta^2 M < 0$, the star is unstable. In the mass/pressure relation, one finds minima and maxima, where $dM/dp_0 = 0$. For these extrema, it can be deduced that also $\delta^2 M = 0$. This means that these extrema are the critical points for stability. The latter condition relates to $\omega^2 = 0$ and therefore signals a change in the stability of the corresponding normal mode.

In the case of multiple critical points, it is also possible that an unstable configuration can change back to stability at the following extremum. Therefore, one has to take into account the sign of the change in the radius R (i.e. $dR/dp_0 < 0$ or $dR/dp_0 > 0$), in addition. If an equilibrium configuration of a star is now transformed from the low-pressure side of the critical point to the high-pressure side, one can find the following relations between the change of the radius R with respect to the central pressure p_0 and the radial oscillation modes:

- $dR/dp_0 < 0$: the square of the oscillation frequency of an even numbered mode changes the sign $\left(\omega_n^2 \to -\omega_n^2\right)$;
- $dR/dp_0 > 0$: the square of the oscillation frequency of an odd numbered mode changes the sign.

For the 'TOV' curve in figure 5, there are three critical points. The first critical point appears at the maximum around $p_0 = 10^{28}$ dyne cm^{-2}. As can be seen in figure 7, dR/dp_0 is negative at this critical point; therefore, an even mode is changing stability. Because of (63) and the assumption that for low densities the oscillation frequencies of all modes are real (i.e. $\omega_n^2 > 0$), ω_0^2 should change its sign here. Therefore, for central pressures between the first critical point and the next one, the oscillation in the fundamental mode is unstable.

At $p_0 \sim 10^{37.5}$ dyne cm^{-2}, the second critical point is reached. Here $dR/dp_0 > 0$ and ω_1^2 becomes negative. At the second maximum at $p_0 \sim 10^{39}$ dyne cm^{-2}, again the oscillation in

an even mode must change the sign and as ω_1^2 is negative already, ω_2^2 becomes negative now. This stability analysis can also be applied to the case of the Newtonian white dwarfs as well as to the neutron stars. As mentioned before, the sequence can become stable again; then at the second critical point the fundamental mode changes its sign back and a stable sequence of compact stars starts again. This so-called third family of compact stars appears for a strong first-order phase transition to e.g. quark matter [15–17].

In summary, white dwarfs become unstable as soon as their mass is above the Chandrasekhar mass limit. This is exactly what is happening in the case of a core-collapse supernova explosion. It is quite interesting to see that such an intuitive reasoning already indicates what is happening in real nature.

3. Pure neutron stars

3.1. Non-relativistic polytropic case

In this section, we start looking at pure non-relativistic neutron stars, which are described by an EoS of a Fermi gas of neutrons. In the following, we drop the subscript 'F' for labelling the Fermi momentum due to practical reasons. With the neutron number density

$$n_{\mathrm{n}} = \frac{k_{\mathrm{n}}^3}{3\pi^2\hbar^3} \tag{66}$$

and the mass density

$$\rho = n_{\mathrm{n}} \cdot m_{\mathrm{n}}, \tag{67}$$

we get in analogy to the Fermi gas for electrons (see equations (17)–(22))

$$\epsilon(x) = \frac{\epsilon_0}{8}[(2x^3 + x)(1 + x^2)^{1/2} - \sinh^{-1}(x)], \tag{68}$$

$$p(x) = \frac{\epsilon_0}{24}[(2x^3 - 3x)(1 + x^2)^{1/2} + 3\sinh^{-1}(x)], \tag{69}$$

with

$$x = \frac{k_{\mathrm{n}}}{m_{\mathrm{n}}c}, \qquad \epsilon_0 = \frac{m_{\mathrm{n}}^4 c^5}{\pi^2\hbar^3}. \tag{70}$$

In the non-relativistic case, equations (68) and (69) simplify to

$$\epsilon(x) \simeq \rho c^2 = \frac{\epsilon_0}{3}x^3, \qquad p(x) \simeq \frac{\epsilon_0}{15}x^5. \tag{71}$$

Hence, the EoS can be described by a polytrope

$$p(\epsilon) = K_{\text{non-rel}}\epsilon^{5/3}, \tag{72}$$

with

$$K_{\text{non-rel}} = \frac{\hbar^2}{15\pi^2 m_{\mathrm{n}}}\left(\frac{3\pi^2}{m_{\mathrm{n}}c^2}\right)^{5/3} = 6.428 \times 10^{-26}\ \text{cm}^2\ \text{erg}^{-2/3}. \tag{73}$$

We start our numerical calculation with our Newtonian code and the results are plotted in figure 8. We arrive at neutron star masses of around $0.5M_\odot$ and radii of 20–30 km. The general relativistic effects for neutron stars should be larger than those for the white dwarfs. In figure 8, we compare the Newtonian with the TOV code results. We see that the general
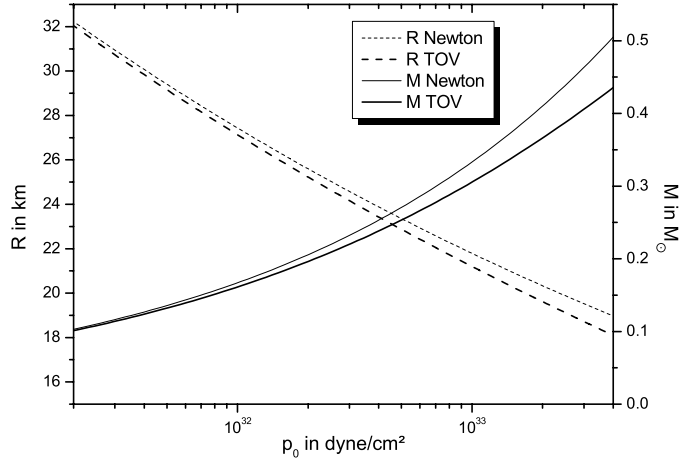
Figure 8. The mass M and the radius R of neutron stars in the non-relativistic case as a function of the central pressure p_0. The results from the TOV equation are compared to the Newtonian limit.

relativistic corrections are at the order of a few per cent and become more and more pronounced for more massive neutron stars.

3.2. Ultra-relativistic polytropic case

For the ultra-relativistic limit, $x \gg 1$, one finds for the energy density and for the pressure of nucleons,

$$\epsilon(x) = \frac{\epsilon_0}{4}x^4, \qquad p(x) = \frac{\epsilon_0}{12}x^4 \quad \Rightarrow \quad p = \epsilon/3, \tag{74}$$

which is similar to the case of ultra-relativistic electrons discussed before. However, the numerical integration of the TOV equations fails here: the condition for terminating the integration ($p \leqslant 0$) cannot be reached. The pressure converges monotonically as a function of the radius against zero, so that the radius of the star approaches infinity. The mass does not go to infinity because $\mathrm{d}m/\mathrm{d}r$ also reaches zero asymptotically. The problem with the relativistic case is that its solution has some principal inconsistencies. Running from the initial pressure p_0 to zero through the whole star, the pressure has to pass the region where neutrons become non-relativistic, necessarily. The pure relativistic approximation is not valid for the whole density range of a compact star.

3.3. Full relativistic case

It is essential to find an equation of state which is valid over the whole range of pressure and energy density. In other words, equations (68) and (69) should be used for the calculation. Again we use a root-finding routine, as we have no explicit equation of state of the form $p(\epsilon)$ or $\epsilon(p)$ anymore. The results for $R(p_0)$ and $M(p_0)$ are shown in figure 9.

The mass–radius relation $M(R)$ is plotted in figure 10, where the maximum mass can easily be recognized. The heaviest stable pure neutron star has a central pressure of $p_0 = 3.5 \times 10^{35}$ dyne cm^{-2}, a mass of $M = 0.712M_\odot$ and a radius of $R = 9.14$ km as first calculated by Oppenheimer and Volkoff in 1939 [18] (they arrived at a maximum mass of $M = 0.71M_\odot$ and a radius of $R = 9.5$ km for comparison).
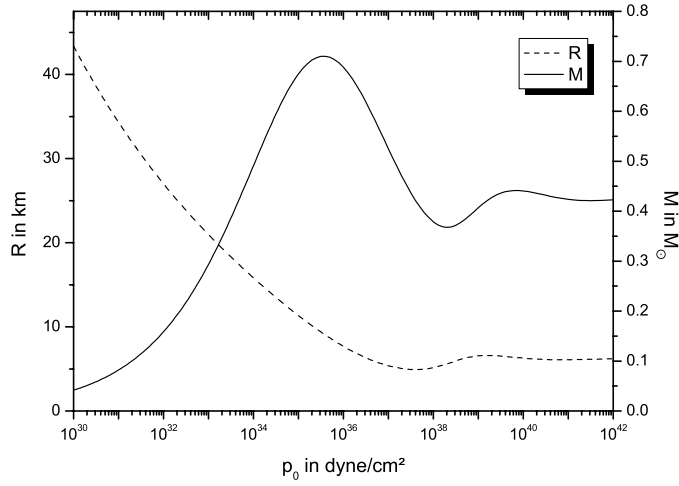
Figure 9. The mass M and the radius R as a function of the central pressure p_0 for pure neutron stars.
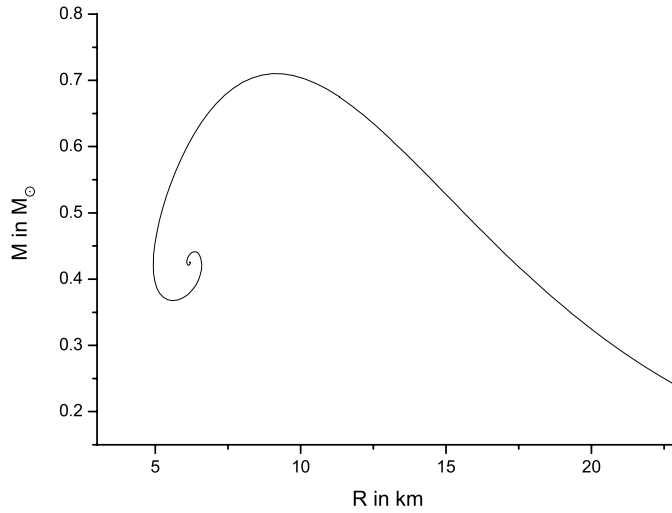

Figure 10. The mass M for pure neutron stars as a function of radius R. The maximum mass is $M = 0.712 M_\odot$ at a radius of $R = 9.14$ km.

4. Neutron stars with protons and electrons

Because the neutron is unstable, a neutron star will not consist of neutrons only, but in addition a finite fraction of protons and electrons will appear in dense matter. The electrons and protons are produced by β-decay:

$$n \longrightarrow p + e^- + \bar{\nu}_e. \tag{75}$$

There exist reverse reactions also, so that an electron and a proton scatter into a neutron and a neutrino:

$$p + e^- \longrightarrow n + \nu_e. \tag{76}$$

As all reactions are in chemical equilibrium, for a cold neutron star, the following relation for the chemical potentials holds:

$$\mu_n = \mu_p + \mu_e. \tag{77}$$

Neutrinos do not have a finite chemical potential ($\mu_\nu = 0$), as the neutrinos escape from the cold star without interactions. Due to stability reasons (see e.g. [14]), it is assumed that the whole neutron star is electrically neutral; hence,

$$n_p = n_e \quad \Leftrightarrow \quad k_p = k_e \tag{78}$$

and the Fermi momenta of protons and electrons must be equal. With the definition of the chemical potential for an ideal Fermi gas with zero temperature,

$$\mu_i(k_i) = \frac{d\epsilon_i}{dn_i} = \left(k_i^2 c^2 + m_i^2 c^4\right)^{1/2}, \qquad i = n, p, e, \tag{79}$$

and using equations (77) and (78), one arrives at the following relation:

$$\left(k_n^2 c^2 + m_n^2 c^4\right)^{1/2} - \left(k_p^2 c^2 + m_p^2 c^4\right)^{1/2} - \left(k_p^2 c^2 + m_e^2 c^4\right)^{1/2} = 0. \tag{80}$$

This equation can be solved for the Fermi momenta of protons k_p as a function of the Fermi momenta of neutrons k_n:

$$k_p(k_n) = \frac{\left[\left(k_n^2 c^2 + m_n^2 c^4 - m_e^2 c^4\right)^2 - 2m_p^2 c^4\left(k_n^2 c^2 + m_n^2 c^4 + m_e^2 c^4\right) + m_p^4 c^8\right]^{1/2}}{2c\left(k_n^2 c^2 + m_n^2 c^4\right)^{1/2}}. \tag{81}$$

The total energy and pressure are now the sum of the energy and pressure of electrons, protons and neutrons, respectively:

$$\epsilon_{tot} = \sum_{i=n,p,e} \epsilon_i, \qquad p_{tot} = \sum_{i=n,p,e} p_i, \tag{82}$$

where

$$\epsilon_i(k_i) = \frac{8\pi}{(2\pi\hbar)^3} \int_0^{k_i} \left(k^2 c^2 + m_i^2 c^4\right)^{1/2} k^2 \, dk, \tag{83}$$

$$p_i(k_i) = \frac{1}{3} \frac{8\pi}{(2\pi\hbar)^3} \int_0^{k_i} \left(k^2 c^2 + m_i^2 c^4\right)^{-1/2} k^4 \, dk. \tag{84}$$

For the case when there are no neutrons present, i.e. $k_n = 0$, equation (81) gives

$$k_p(0) = \frac{\left[\left(m_n^2 c^4 - m_e^2 c^4\right)^2 - 2m_p^2 c^4\left(m_n^2 c^4 + m_e^2 c^4\right) + m_p^4 c^8\right]^{1/2}}{2m_n c^3} = 1.264 \times 10^{-3} m_n c. \tag{85}$$

This means that equation (81) can only be used if $k_p > 1.264 \times 10^{-3} m_n c$, which is fulfilled for $p > p_{crit} = 3.038 \times 10^{24}$ dyne cm^{-2}. Below this pressure, no neutrons are present anymore, so the 'neutron star' material consists of protons and electrons only. Figure 11 shows the equation of state for a free gas of protons, electrons and neutrons in β-equilibrium in the form $\epsilon(p)$. Around the critical pressure, a notable kink appears in the equation of state, which can be identified with the strong onset of neutrons appearing in matter with their corresponding additional contribution to the energy density. (One can show that $\frac{d^2\epsilon}{dp^2}\big|_{p_{crit}} = \infty$, but $\frac{d\epsilon}{dp}\big|_{p_{crit}}$ is continuous and thus the physical situation is not that of a true thermodynamic phase transition.)

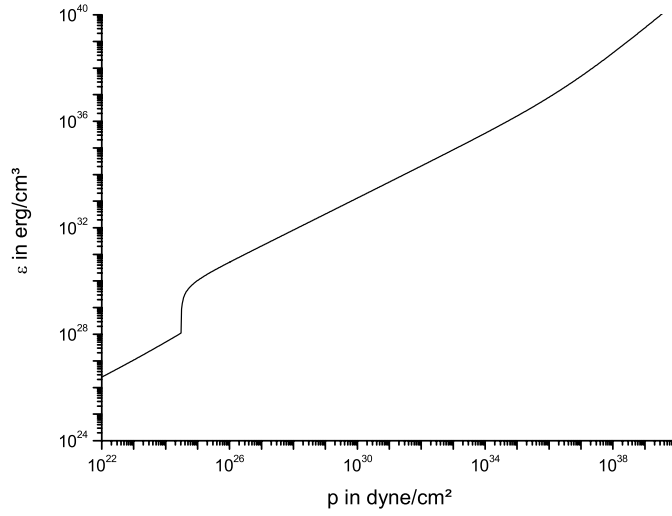**Figure 11.** The energy density ϵ as a function of the pressure p for neutron stars including protons and electrons. At $p = 3 \times 10^{24}$ dyne cm^{-2}, neutrons begin to appear.
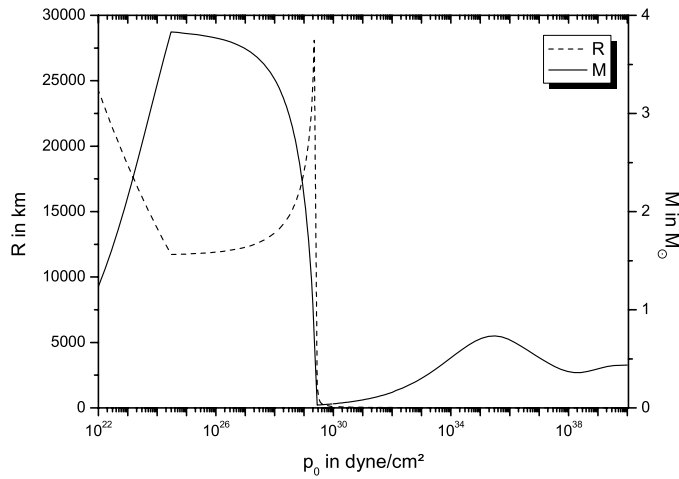

Figure 12. The mass M and the radius R as a function of the central pressure p_0 for neutron stars including protons and electrons.

Using the new equation of state, we start our TOV calculation and compute masses and radii which are depicted in figures 12 and 14, respectively. The result seems to be surprising at first glance but can be explained by looking at the proton-to-nucleon fraction integrated over every single star as displayed in figure 13.

Below the critical pressure of $p = 3.038 \times 10^{24}$ dyne cm^{-2}, the neutron star consists of protons and electrons only by definition. Above this pressure, neutrons appear, resulting in a sharp bend of $M(p_0)$ and $R(p_0)$. Between the critical pressure and $p \simeq 10^{29}$ dyne cm^{-2}, the stars have a tiny neutron fraction in the core, which increases with the pressure. The increasing neutron fraction is responsible for the decreasing masses. On the microscopic
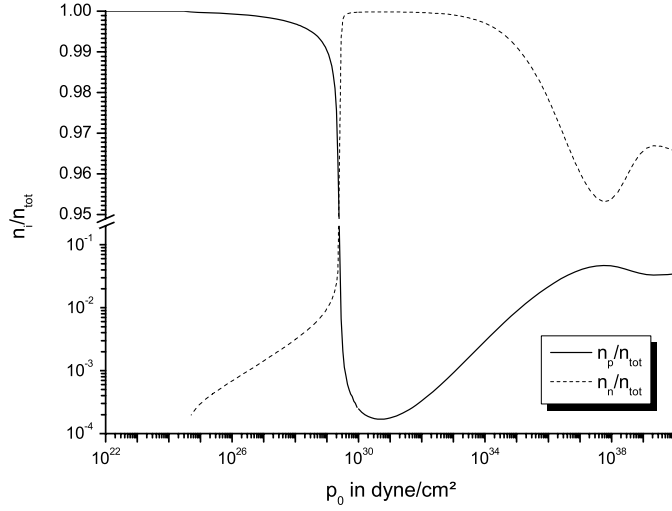
Figure 13. The proton-to-nucleon fraction n_p/n_{tot} and the neutron-to-nucleon fraction n_n/n_{tot}, integrated over every single star, versus the central pressure p_0.
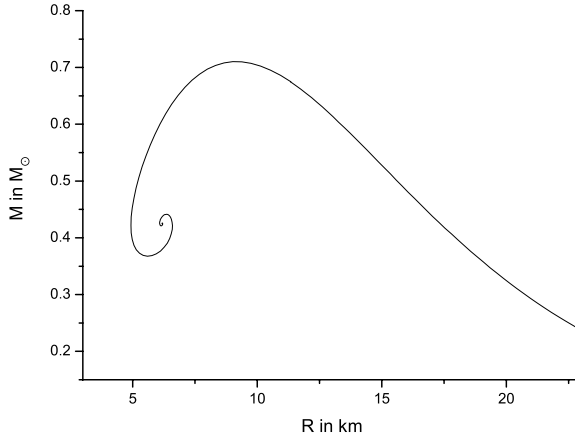

Figure 14. The mass M as a function of the radius R for neutron stars including protons and electrons. The maximum mass star has a mass of $M = 0.699 M_\odot$, the corresponding radius is $R = 9.24$ km.

scale, the relativistic electrons combine with the protons to form neutrons, thereby reducing the electron degeneracy pressure. For the same energy density, the pressure will be lower, if neutron production is included, so only a smaller mass is supported by the star. At $p \simeq 10^{30}$ dyne cm^{-2}, the proton fraction drops to $n_p/n_{tot} \leqslant 10^{-3}$ and the star becomes an almost pure neutron star (hence the name). The proton fraction is so small that it can be safely neglected. As a consequence, the stellar objects become more compact, with a smaller radius and mass. For larger pressures ($p > 10^{30}$ dyne cm^{-2}), the mass increases again with rising pressure. The neutrons start to become degenerate; the star is stable because of the neutron degeneracy pressure.
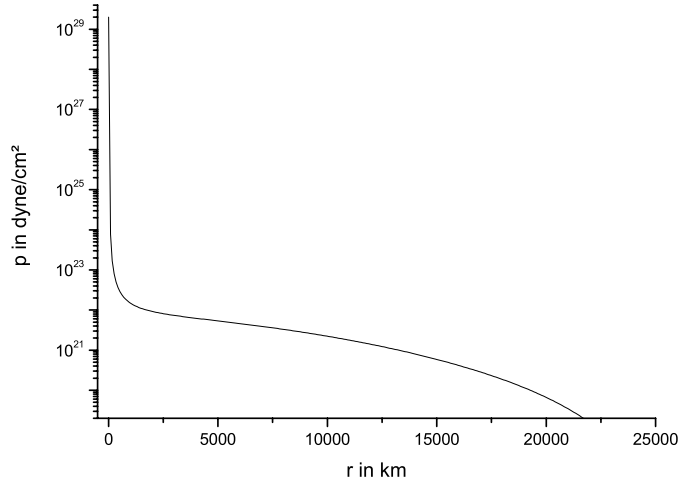
Figure 15. The pressure p along the radius r for a single neutron star including protons and electrons at $p_0 = 2 \times 10^{29}$ dyne cm^{-2}.

So the behaviour of $M(p_0)$ is understood through the change of the proton fraction $n_p/n_{tot}(p_0)$. But what about the unusual peak of $R(p_0)$? Similar to the ultra-relativistic description of a pure neutron star, the situation at $p_0 \simeq 10^{29}$ dyne cm^{-2} is that the pressure approaches zero very slowly, but never reaches it or falls below. Figure 15 shows a star with $p_0 = 2 \times 10^{29}$ dyne cm^{-2}, where this behaviour can be seen clearly. So it is necessary to make a cut-off (for this case at $p = 10^{19}$ dyne cm^{-2}), so that the integration terminates as soon as this pressure is reached. During the numerical computation, the mass converges to M, while the radius grows bigger and bigger. This neutron star consists of a dense central core and a huge low-density crust. The protons and electrons are responsible for these huge radii: the energy density for the same pressure is much lower, if no neutrons are present (see figure 11). Because $\mathrm{d}p/\mathrm{d}r$ (equation (53)) is a function of the energy density ϵ, the pressure $p(r)$ inside a star will decrease much more slowly if there are only protons and electrons left. For more massive stars, this crust disappears and the radius is determined by the neutron core. After all, such a huge crust does not seem to be very realistic for neutron stars.

Note that for the most compact neutron stars (i.e. for $p_0 > 10^{34}$ dyne cm^{-2}) protons appear again. The proton fraction approaches a certain constant limit at high densities. Using equation (81) in the ultra-relativistic limit, $k_n c \gg m_n c^2$, results in

$$k_p(k_n) \approx 1/2 k_n \Longrightarrow n_p = 1/8 n_n \tag{86}$$

$$\Longrightarrow \frac{n_p}{n_{tot}} = \frac{n_p}{n_p + n_n} = \frac{1}{9}. \tag{87}$$

The proton fraction for large p_0 in figure 13 is of course smaller than $1/9$, as only the central core obeys the relativistic limit, and no protons are present for the regions in the star with smaller pressure. The maximum mass star has a proton fraction of $n_p/n_{tot} \simeq 0.02$.

Another important point is that all stars in the region of 10^{24} dyne cm$^{-2} < p_0 < 10^{29}$ dyne cm^{-2} are unstable, which can be seen from the M versus p_0 plot in figure 12. Hence, there are only two different kinds of stable objects: first the 'hydrogen white dwarfs', like stars consisting of protons and electrons, up to $M = 4M_\odot$ and with radii of about 10^4 km,

then the almost pure neutron stars with a maximum mass of $M = 0.699 M_\odot$ and a radius $R = 9.24$ km at a central pressure $p_0 = 3.412 \times 10^{35}$ dyne cm^{-2}. Compared to $M = 0.712 M_\odot$ and $R = 9.14$ km for the pure neutron star of the last section, the differences are quite small. The minimum neutron star mass is found to be about $0.03 M_\odot$ with a radius of around 1000 km; the radius rapidly changes for this mass range and quickly shrinks to values of 200–300 km for slightly larger masses. We note that these values for the minimum mass of neutron stars are not far from the result of $M_{\min} = 0.09 M_\odot$ found in more elaborate calculations (see e.g. [19]).

5. Models for the nuclear interactions

5.1. Empirical interaction

In this and the following section, we use MeV and fm for the energy and distance units. Additionally, c is set to 1 and $\hbar c = 197.3$ MeV fm.

Following [1], we introduce an empirical interaction for symmetric matter ($n_n = n_p$) of the form (see also [20])

$$\frac{\epsilon(n)}{n} = m_N + \langle E_0 \rangle u^{2/3} + \frac{A}{2} u + \frac{B}{\sigma + 1} u^\sigma, \qquad u = n/n_0, \tag{88}$$

where n denotes the total nucleon number density of the system.

The dimensionless quantity σ and the quantities A and B with dimension of MeV are the fit parameters of the model. In fact, only the third and the fourth term of equation (88) describe interaction terms, $\langle E_0 \rangle$ is the average kinetic energy per nucleon of symmetric matter in its ground state:

$$\langle E_0 \rangle = \frac{3}{5} \frac{k_0^2}{2m_N} = \frac{3}{5} \frac{1}{2m_N} \left(\frac{3\pi^2 \hbar^3 n_0}{2} \right)^{2/3}. \tag{89}$$

The factor 2 in the denominator of the parentheses comes in as an additional degeneration factor for the isospin (compare to equation (13)).

In the model, the following values should be reproduced by the ansatz of equation (88):

- the equilibrium number density $n_0 = 0.16$ nucleons fm^{-3} $\Longrightarrow k_0 = 263$ MeV;
- the average binding energy per nucleon BE $= (E/A - m_N)|_{n=n_0} = (\epsilon(n)/n - m_N)|_{n=n_0} = -16$ MeV;
- the nuclear compressibility in nuclear matter $K(n_0) = 9\frac{\mathrm{d}p(n)}{\mathrm{d}n}\big|_{n=n_0} = 400$ MeV.

After some algebra, one gets the following parameters:

$$A = -118.2 \text{ MeV}, \quad B = 65.39 \text{ MeV}, \quad \sigma = 2.112, \quad \langle E_0 \rangle = 22.1 \text{ MeV}. \tag{90}$$

For known $\epsilon(n)$, it is possible to determine $p(n)$ via

$$p(n) = n^2 \frac{\mathrm{d}}{\mathrm{d}n}\left(\frac{\epsilon}{n} \right) = n_0 \left[\frac{2}{3} \langle E_0 \rangle u^{5/3} + \frac{A}{2} u^2 + \frac{B\sigma}{\sigma + 1} u^{\sigma+1} \right]. \tag{91}$$

We proceed now to extrapolate to asymmetric nuclear matter.

First, the neutron-to-proton ratio is expressed through a parameter α:

$$\alpha = \frac{n_n - n_p}{n} = \frac{N - Z}{A}. \tag{92}$$

Now the kinetic energy is given by the sum of the kinetic energies of protons and neutrons:

$$\epsilon_{\mathrm{KE}}(n, \alpha) = \frac{3}{5} \frac{k_{\mathrm{n}}^2}{2m_{\mathrm{N}}} n_{\mathrm{n}} + \frac{3}{5} \frac{k_{\mathrm{p}}^2}{2m_{\mathrm{N}}} n_{\mathrm{p}} \tag{93}$$

$$= n\langle E_{\mathrm{F}}\rangle \frac{1}{2}[(1 + \alpha)^{5/3} + (1 - \alpha)^{5/3}], \tag{94}$$

$$\langle E_{\mathrm{F}}\rangle = \frac{3}{5} \frac{1}{2m_{\mathrm{N}}} \left(\frac{3\pi^2 \hbar^3 n}{2}\right)^{2/3}. \tag{95}$$

The difference in the kinetic energy density relative to the symmetric case can be expressed as a function of n and α:

$$\Delta\epsilon_{\mathrm{KE}}(n, \alpha) = \epsilon_{\mathrm{KE}}(n, \alpha) - \epsilon_{\mathrm{KE}}(n, 0)$$

$$= n\langle E_{\mathrm{F}}\rangle\left\{\tfrac{1}{2}\left[(1 + \alpha)^{5/3} + (1 - \alpha)^{5/3}\right] - 1\right\}. \tag{96}$$

This gives the following Taylor approximation:

$$\Delta\epsilon_{\mathrm{KE}}(n, \alpha) = n\langle E_{\mathrm{F}}\rangle \frac{5}{9}\alpha^2 \left(1 + \frac{\alpha^2}{27} + \cdots\right). \tag{97}$$

This mean that it is sufficient to keep corrections of order α^2:

$$\frac{E(n, \alpha)}{A} = \frac{E(n, 0)}{A} + \alpha^2 S(n). \tag{98}$$

The function $S(u)$, which describes the symmetry energy, is assumed to have the following form:

$$S(u) = (2^{2/3} - 1)\langle E_0\rangle(u^{2/3} - F(u)) + S_0 F(u). \tag{99}$$

S_0 is an input parameter (the asymmetry energy), which describes the energy difference between pure neutron matter and normal symmetric nuclear matter at ground-state density n_0. In the following calculations, S_0 is set to 30 MeV. The only restrictions to the function $F(u)$ are $F(1) = 1$ and $F(0) = 0$, in order to satisfy $S(1) = S_0$ and $S(0) = 0$, respectively. Besides this, $F(u)$ can be chosen freely. We make the straightforward choice

$$F(u) = u. \tag{100}$$

The factor $(2^{2/3} - 1)\langle E_0\rangle$ can be explained as follows. For pure neutron matter, $\alpha = 1$, the kinetic energy is not given by equation (89) anymore, the factor 2 in the denominator of the parentheses has to drop out. The factor $(2^{2/3} - 1)\langle E_0\rangle$ takes this into account:

$$\frac{E(n, 1)}{A} = m_{\mathrm{N}} + \langle E_0\rangle u^{2/3} + \frac{A}{2}u + \frac{B}{\sigma + 1}u^\sigma + (2^{2/3} - 1)\langle E_0\rangle(u^{2/3} - F(u)) + S_0 F(u)$$

$$= m_{\mathrm{N}} + \langle E_0\rangle u^{2/3} + (2^{2/3} - 1)\langle E_0\rangle u^{2/3} + \frac{A}{2}u + \frac{B}{\sigma + 1}u^\sigma + (S_0 - (2^{2/3} - 1)\langle E_0\rangle)F(u)$$

$$= m_{\mathrm{N}} + 2^{2/3}\langle E_0\rangle u^{2/3} + \frac{A}{2}u + \frac{B}{\sigma + 1}u^\sigma + (S_0 - (2^{2/3} - 1)\langle E_0\rangle)F(u). \tag{101}$$

Thus, the ansatz of equation (99) implies the correct expression for the kinetic energy of pure neutron matter. Also, the different contributions to the potential energy are separated from each other.

With $\epsilon(n, \alpha) = nE(n, \alpha)/A$, it is straightforward to calculate $p(n, \alpha)$:

$$p(n, \alpha) = n^2 \frac{\mathrm{d}}{\mathrm{d}n}\left(\frac{\epsilon(n, \alpha)}{n}\right)$$

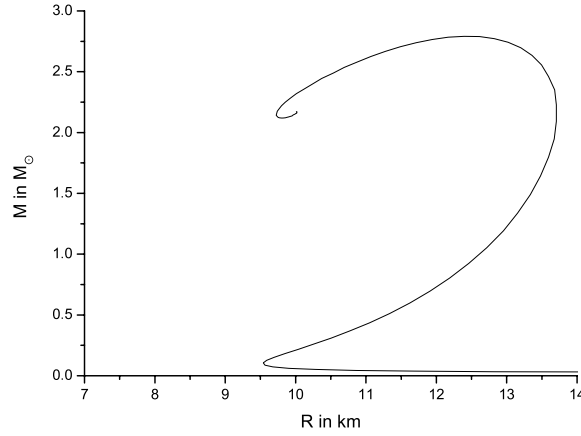$$= p(n, 0) + n_0\alpha^2[(2^{2/3} - 1)\langle E_0\rangle(2/3u^{5/3} - u^2) + S_0 u^2]. \tag{102}$$

Figure 16. The mass M as a function of the radius R for the empirical nucleon–nucleon interaction. The maximum mass star has a mass of $M = 2.792M_\odot$, the corresponding radius is $R = 12.46$ km.

As seen in the previous section, the proton fraction for stable compact stars is small. Hence, the parameter α is set to be equal to 1 and a pure neutron star is considered in the following.

With $p(n)$ and $\epsilon(n)$ given, one can start the numerical computation again. The results are shown in figure 16. The maximum mass star has a mass of $M = 2.792M_\odot$ and a radius of $R = 12.46$ km. The neutron star is much more massive, if nucleon–nucleon interactions are included. As the equation of state is much harder, which means that the pressure increases faster with the energy density, the star can support a much larger mass.

Another interesting fact is the behaviour of the mass for decreasing central pressure. In a certain region, the mass–radius curve drops to smaller radii as the pressure and the mass decrease, until a radius of $R \simeq 9.5$ km and a mass of $M \simeq 0.1M_\odot$ are reached at a central pressure of $p \simeq 1.7 \times 10^{33}$ dyne cm^{-2}. Passing this point, the radius starts to increase again. This special shape is due to the equation of state employed here. In figure 17, one sees that the EoS differs from those before: there is a smooth bump at $p \simeq 4 \times 10^{31}$ dyne cm^{-2}. For pressures below this value, an increase in the energy density leads to a very small increase in pressure, which is due to the attractive part of the interaction for matter close to the ground-state density. In this pressure region, a higher central pressure can only be generated by a smaller radius at a nearly unchanged mass. The slope of the EoS for pressures greater than the value of $p \simeq 4 \times 10^{31}$ dyne cm^{-2} changes notably, so that also the mass–radius relation for the corresponding neutron stars is affected. For larger pressures, the pressure increases much faster with the energy density, which results in the abrupt rise of the masses (see figure 16). The repulsive force of the interaction becomes dominant for nuclear densities above the ground-state density. Now an increase in energy density leads to a strong increase in pressure also and a larger mass is supported by the star.

In fact, the EoS used here is not valid for small pressures and energy densities. Below nuclear matter density n_0, it is not realistic to use a uniform matter distribution anymore. The formation of a lattice of nuclei and the occurrence of certain possible mixed phases become important in the outer layers, the so-called crust of neutron stars. For pressures below 10^{33} dyne cm^{-2}, one has to use a special equation of state to describe the matter in the crust. Taking into account a realistic EoS for the crust would wash out the bump seen in figure 17 and also the characteristic features in the mass–radius relation described above. A good introduction to neutron star crusts can be found in e.g. [21, 22].
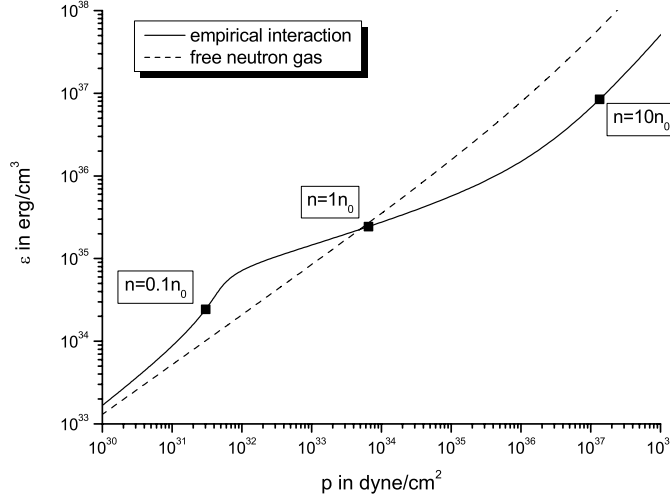
Figure 17. The equation of state for the empirical nucleon–nucleon interaction compared to that of a free neutron gas.

5.2. Skyrme parametrized interaction

In the following, the properties of nuclear matter are considered by applying the Hartree–Fock method on a phenomenological nucleon–nucleon interaction (for further information see also [23]).

Consider a system consisting of N_p protons and N_n neutrons, which are described by plain waves:

$$\varphi_\alpha = \frac{1}{\sqrt{V}} \, e^{ikx} \chi_S \chi_I. \tag{103}$$

Here, χ_I is the degree of freedom for the isospin, χ_S for the spin. The self-consistent Hartree–Fock equations read

$$\epsilon_\alpha \varphi_\alpha(x) = \hat{t}\varphi_\alpha(x) + \sum_{\alpha'} \int d^3y \, \varphi_\alpha^\dagger(y) V(x,y)[\varphi_{\alpha'}(y)\varphi_\alpha(x) - \varphi_\alpha(y)\varphi_{\alpha'}(x)], \tag{104}$$

where $\sum_{\alpha'}$ is the sum over all occupied states. The potential is spin and isospin independent, so the sum can be divided into a part for protons and one for neutrons:

$$\sum_{\alpha'} \cdots = \sum_{k,s}^{k_F^{(p)}} \cdots + \sum_{k,s}^{k_F^{(n)}}. \tag{105}$$

As the sum splits up, one gets a separate Hartree–Fock equation for neutrons and protons,

$$\epsilon_k^{(p)}\varphi_k^{(p)}(x) = \hat{t}\varphi_k^{(p)}(x) + (2s+1)\sum_{k'}^{k_F^{(p)}} \int d^3y \left[\varphi_{k'}^{(p)*}(y)\varphi_{k'}^{(p)}(y)\right] V(x,y)\varphi_k^{(p)}(x)$$

$$-1 \cdot \sum_{k'}^{k_F^{(p)}} \int d^3y \left[\varphi_{k'}^{(p)*}(y)\varphi_k^{(p)}(y)\right] V(x,y)\varphi_{k'}^{(p)}(x)$$

$$+(2s+1)\sum_{k'}^{k_F^{(n)}} \int d^3y \left[\varphi_{k'}^{(n)*}(y)\varphi_{k'}^{(n)}(y)\right] V(x,y)\varphi_k^{(p)}(x), \tag{106}$$

by taking into account the spin degrees of freedom $g_s = 2s + 1$. The neutron wavefunction results from exchanging the superscripts (p) and (n).

Next, the interaction is introduced as a Skyrme-type parametrization:

$$V(x, y) = \delta^3(x - y)\left(\tfrac{1}{6}t_3 n - t_0\right),\tag{107}$$

where t_0 describes the attractive two-particle nuclear interaction, whereas $t_3 n$ describes the repulsive (and density-dependent) many-body interaction which is the dominant one at high nuclear densities. Again, n denotes the total number density of the system:

$$n = (N_n + N_p)/V = n_n + n_p.\tag{108}$$

The single-particle energies for protons and neutrons can then be derived as

$$\epsilon_k^{(p)} = \frac{k_p^2}{2m_p} + \left(\frac{1}{6}t_3 n - t_0\right)\frac{1}{V}(N_p/2 + N_n),$$

$$\epsilon_k^{(n)} = \frac{k_n^2}{2m_n} + \left(\frac{1}{6}t_3 n - t_0\right)\frac{1}{V}(N_n/2 + N_p).\tag{109}$$

The total energy for a homogeneous system is given by

$$E_{HF} = \frac{1}{2}\sum_i^{N_p}\left(\epsilon_i^{(p)} + t_i\right) + \frac{1}{2}\sum_i^{N_n}\left(\epsilon_i^{(n)} + t_i\right)\tag{110}$$

$$\implies E_{HF} = N_p\frac{3}{5}\frac{k_p^2}{2m_p} + N_n\frac{3}{5}\frac{k_n^2}{2m_n} + \frac{1}{2}\left(\frac{1}{6}t_3 n - t_0\right)\frac{1}{V}\left(N_p^2/2 + 2N_p N_n + N_n^2/2\right).\tag{111}$$

The next task is to determine the phenomenological parameters t_0 and t_3. For $n = n_0 = 0.16$ fm^3, the total energy shall have a minimum with $E_{HF}/A = BE = -16$ MeV. From these conditions, one arrives at

$$t_3 = \frac{16E_B}{n_0^2} + \frac{8}{5}\frac{(\hbar c)^2}{m_n c^2}\left(\frac{3\pi^2}{2}\right)^{2/3}(n_0)^{-4/3},$$

$$t_0 = \frac{16E_B}{3n_0} + \frac{16}{15}\frac{(\hbar c)^2}{m_n c^2}\left(\frac{3\pi^2}{2}\right)^{2/3}(n_0)^{-1/3}\tag{112}$$

$$\implies t_0 = 1024.1 \text{ MeV fm}^3, \qquad t_3 = 14\,600.8 \text{ MeV fm}^6.\tag{113}$$

With

$$K(n_0) = 9\frac{dp(n)}{dn}\bigg|_{n=n_0},\tag{114}$$

one finds a value of 376.4 MeV for the nuclear compressibility, which is less than that for the empirical interaction.

Again, we assume pure neutron matter, i.e. we set $N_p = 0$ and $N_n = A$:

$$\frac{E_{HF}}{A} = \frac{3}{5}\frac{k_n^2}{2m_n} + \frac{1}{4}\left(\frac{1}{6}t_3 n - t_0\right)n.\tag{115}$$

With the total energy density $\epsilon(n)$, including the rest mass term $m_n \cdot n$,

$$\epsilon(n) = (m_n + E_{HF}/A)\cdot n\tag{116}$$

$$= m_n n + \frac{3}{10m_n}(3\pi^2\hbar^3)^{2/3}n^{5/3} + \frac{t_3}{24}n^3 - \frac{t_0}{4}n^2,\tag{117}$$
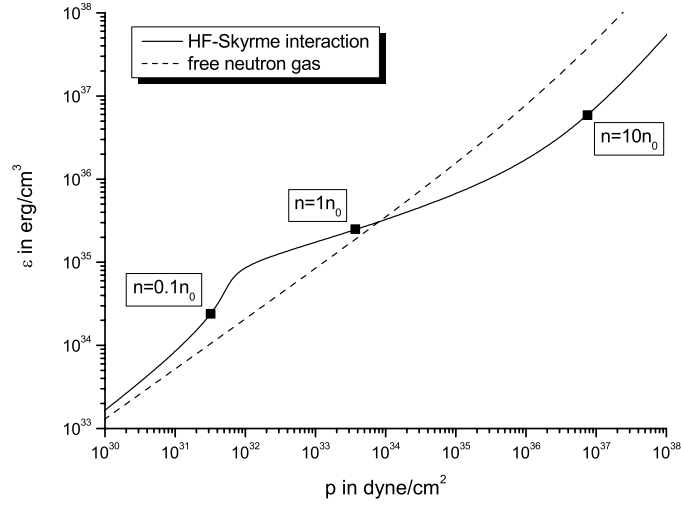
Figure 18. The equation of state for the Skyrme parametrization and for a free neutron gas.
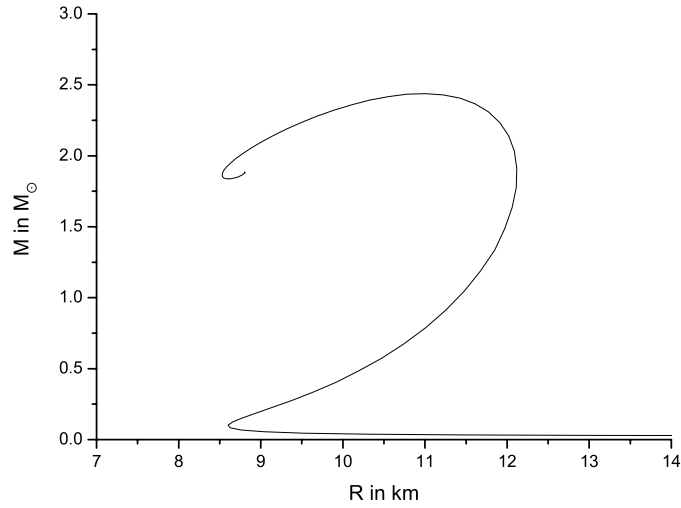

Figure 19. The mass M as a function of R for the Skyrme parametrization. The maximum mass star has a mass of $M = 2.438 M_\odot$ and a radius of $R = 10.98$ km.

one can derive $p(n)$ according to the thermodynamic relation

$$p(n) = n\frac{\mathrm{d}}{\mathrm{d}n}\epsilon(n) - \epsilon(n) \tag{118}$$

$$\implies p(n) = \frac{2}{10 m_n}(3\pi^2\hbar^3)^{2/3}n^{5/3} + \frac{t_3}{12}n^3 - \frac{t_0}{4}n^2. \tag{119}$$

The resulting equation of state is plotted in figure 18, which appears to be very similar to the empirical interaction discussed before.

Figure 19 depicts the corresponding mass–radius plot. The maximum mass star has a mass of $M = 2.438M_\odot$ and a radius of $R = 10.98$ km. These values are only a bit smaller than those calculated before for the empirical interaction, also the shape of the curve looks similar. The sharp turnover in the lower left corner of the plot corresponds to a minimal radius of only $R \simeq 8.6$ km and a mass of $M \simeq 0.1M_\odot$.

5.3. Comparing the two models

It is instructive to take a closer look at the two different EoSs considered here, as the results do not differ that much from each other. The two energy densities (equations (98) and (117)) are

- empirical nucleon–nucleon parametrization:

$$\frac{\epsilon_{\mathrm{emp}}(n)}{n} = m_{\mathrm{n}} + \langle E_0 \rangle u^{2/3} + \frac{A}{2}u + \frac{B}{\sigma+1}u^\sigma + (2^{2/3}-1)\langle E_0 \rangle(u^{2/3}-u) + S_0 u; \qquad (120)$$

- Hartree–Fock method and Skyrme parametrization:

$$\frac{\epsilon_{\mathrm{HF}}(n)}{n} = m_{\mathrm{n}} + \frac{3}{10m_{\mathrm{n}}}(3\pi^2\hbar^3)^{2/3}n^{2/3} + \frac{1}{4}\left(\frac{1}{6}t_3 n - t_0\right)n. \qquad (121)$$

With $n = u \cdot n_0$ and equation (89), one can rewrite the two equations in the following form:

$$\frac{\epsilon_{\mathrm{emp}}(n)}{n} = m_{\mathrm{n}} + 2^{2/3}\langle E_0 \rangle u^{2/3} + \left(\frac{A}{2} - (2^{2/3}-1)\langle E_0 \rangle + S_0\right)u + \frac{B}{\sigma+1}u^\sigma, \qquad (122)$$

$$\frac{\epsilon_{\mathrm{HF}}(n)}{n} = m_{\mathrm{n}} + 2^{2/3}\langle E_0 \rangle u^{2/3} - \frac{1}{4}t_0 n_0 u + \frac{1}{24}t_3 n_0^2 u^2. \qquad (123)$$

By inserting the numbers (113), the energy density exhibits the following parametric form:

$$\frac{\epsilon_{\mathrm{emp}}(n)}{n} = (939.6 + 35.1u^{2/3} - 42.1u + 21.0u^{2.112})\ \mathrm{MeV} \xrightarrow{u \gg 1} 21.0u^{2.112}\ \mathrm{MeV}, \qquad (124)$$

$$\frac{\epsilon_{\mathrm{HF}}(n)}{n} = (939.6 + 35.1u^{2/3} - 41.0u + 15.6u^2)\ \mathrm{MeV} \xrightarrow{u \gg 1} 15.6u^2\ \mathrm{MeV}. \qquad (125)$$

If the energy density follows a power law as a function of n, it is easy to find an explicit equation of state of the form $p(\epsilon)$:

$$\begin{aligned} \epsilon &= c \cdot n^k, \\ p &= n \cdot \frac{\mathrm{d}\epsilon}{\mathrm{d}n} - \epsilon = (k-1)c \cdot n^k, \\ p(\epsilon) &= (k-1)\epsilon. \end{aligned} \qquad (126)$$

In our case, $k = 3.112$ for the empirical interaction and $k = 3$ for the Skyrme parametrization. One can see that the first EoS is stiffer than the second. This explains why the masses in the empirical model are larger than the masses in the Skyrme parametrization; the harder EoS can support more mass.
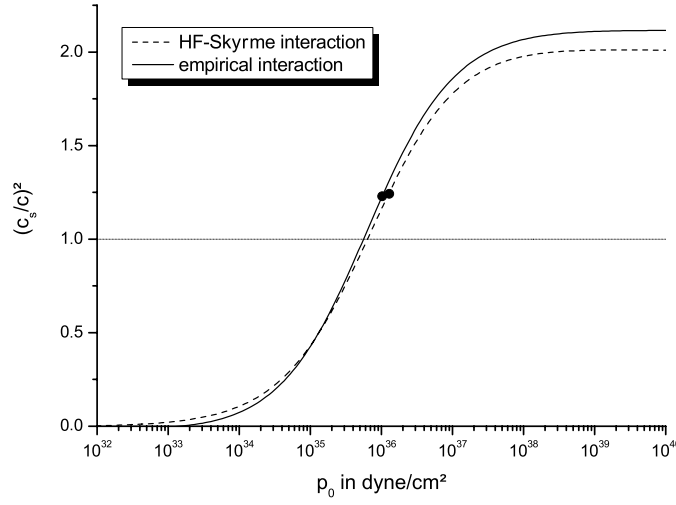
Figure 20. The speed of sound depending on the central pressure for the two different models. The maximum mass stars are marked with a dot.

5.4. Speed of sound and causality

The speed of sound in our neutron star must be less than the speed of light to fulfil relativistic causality. The adiabatic speed of sound is given by $c_s = \frac{dp}{d\epsilon}$ in a non-dispersive medium. Hence, we have

$$1 \leqslant \left(\frac{c_s}{c}\right)^2 = \frac{dp}{d\epsilon} = \frac{dp/dn}{d\epsilon/dn}. \tag{127}$$

Using equation (126), one gets

$$\frac{dp}{d\epsilon} = k - 1 \leqslant 1. \tag{128}$$

Hence, the power coefficient k must be less than or equal to 2. So both EoSs will become acausal for large n. This behaviour is demonstrated in figure 20, where the speed of sound is plotted against the central pressure. As one can see, for the maximum mass star the speed of sound c_s/c is larger than 1 for both interactions considered. Hence, correction factors have to be added to the interaction, which include (or simulate) relativistic effects (see e.g. [24]).

6. Summary and brief overview of present-day developments

In section 2, we discussed the common structure equations for stars as well as the relativistic and non-relativistic equations of state (EoSs) for a Fermi gas of electrons and nucleons. We simplified the EoS to a polytropic form and derived semi-analytically the Chandrasekhar mass limit of $M = 1.4312(2/\eta)^2 M_\odot$ for white dwarfs. We calculated numerically mass–radius relations for white dwarfs using the relativistic and non-relativistic polytropic approximations. For the relativistic case, we find the computed masses to be constant and in very good agreement with the Chandrasekhar mass limit. The numerical results were also checked by the analytical results for white dwarf radii.

We introduced a numerical method to calculate the EoS of a free gas of particles for the general case, i.e. without using the polytropic approximation, and computed the corresponding

masses and radii for white dwarfs. In this case, the calculated masses became larger with increasing central pressures up to a maximum mass of around $1.4M_\odot$. For high pressures, the masses stayed constant at the maximum value showing that the EoS turned into a relativistic polytrope.

We calculated the mass–radius relations without as well as with corrections from general relativity. The mass curve showed an increasing mass for larger central pressures up to $p_0 \sim 10^{28}$ dyne cm^{-2} reaching a maximum mass of about $1.40M_\odot$ without and one of $1.39M_\odot$ with relativistic corrections. The slightly reduced maximum mass in the latter case was in accord with the fact that general relativity corrections strengthen the gravitational force.

We also discussed that white dwarfs and neutron stars are stable against radial oscillations for masses smaller than the maximum mass but unstable beyond the mass peak.

In section 3, we looked at pure neutron stars using an EoS of a free Fermi gas of neutrons. We computed the exact equation of state by a root-finding routine. The maximum mass for such a neutron star was found to be $M = 0.712M_\odot$ with a radius of $R = 9.14$ km. Then, we included protons and electrons in β-equilibrium to the composition of neutron star matter. As the proton fraction was found to be small, the maximum mass of the corresponding neutron star changed only slightly to $M = 0.699M_\odot$ and the radius to $R = 9.24$ km.

Next, we focused on the impact of nuclear interactions on the properties of pure neutron stars. We analysed two different types of interaction, an empirical interaction and the Hartree–Fock method applied to a Skyrme parametrization. As the two resulting EoSs were very close to each other, the results for the mass and radius curves were very similar, but quite different to the cases of free Fermi gases considered before. The maximum masses of neutron stars reached values of $M = 2.4M_\odot$ and $M = 2.8M_\odot$, respectively, which were up to four times larger than those for the free cases. The corresponding radii increased to $R = 11$–12 km, respectively. The repulsion between nucleons stiffened the EoS, increased the pressure at a fixed energy density and enabled stabilization of more massive neutron stars compared to the free Fermi gas case. Caveats of the simple nuclear interaction models used were exhibited, as the neglect of relativistic effects and the EoSs becoming acausal for large central pressures.

We end this section with a brief discussion of present-day developments in the field of compact stars: astrophysical data, the EoS of dense matter and its impact on the global properties of compact stars (for a recent general introduction on the latest developments in the field, we refer to [25]).

More than 1500 pulsars, rotating neutron stars with pulsed radio emission, are known today. About seven thermally emitting isolated neutron stars have been observed by the Hubble Space Telescope (HST), by the x-ray satellites Chandra and XMM-Newton and by ground-based optical telescopes such as the European Southern Observatory (ESO). For the closed and best studied one, RX J1856.5-3754, the measured spectra can be well described by a Planck curve [26]. As the outermost layer of a neutron star is the atmosphere up to a density of 10^4 g cm^{-3} consisting of atoms, their presence should show up in the spectra. However, there is a lack of any atomic spectral line in the spectra which is not understood at present [27]. For three selected rotating neutron stars (pulsars), nicknamed the Three Musketeers, one is even able to make phase-resolved studies of the spectra, which allows us to determine that there are hot spots on the surface of the neutron star [28].

The high-density EoS for neutron stars and the appearance of exotic matter have been studied in modern relativistic field-theoretical models [14]. In particular, hyperons will appear around twice normal nuclear matter density (see e.g. [29] and references therein). The possibility of Bose condensation of kaons in dense, cold matter has also been investigated [30]. Last but not the least, the phase transition to strange quark matter, quark matter with strange quarks, will appear in the high-density limit [31, 32]. If the phase transition of these

exotic forms of matter is strongly first order, a new class of compact stars emerges as a new stable solution of the TOV equations. While the existence of this third family of compact stars besides white dwarfs and neutron stars was known earlier [15, 33, 34], the solution was rediscovered in modern models for the EoS and a Gibbs phase transition only recently [16, 17, 35, 36]. The topic of the third family of compact stars was a subject for another undergraduate student project of Jean Macher and one of the authors [37]. The study of dense quark matter, as possibly present in the core of neutron stars, has been the object of intense investigation during the last few years due to the rediscovery of the phenomenon of colour superconductivity. Here, two colour charged quarks form a (colour) superconducting state and change the properties of quark matter (for reviews, see e.g. [38–40]). Neutron stars with colour superconducting quark matter have been calculated by many authors in the last couple of years; see [41–51]. The physics of strange quark matter in compact stars and its possible signals were reviewed most recently in [31, 32].

The physics of the neutron star also has impact not only on pulsars but also on other active research fields of astrophysics. For example, in x-ray binaries, a neutron star accretes matter from its companion, which is an ordinary star or a white dwarf. When the matter falls onto the neutron star, x-ray bursts occur. Red-shifted spectral lines have been measured from such x-ray binaries, which allow one to constrain the compactness and by that the EoS of neutron stars [52]. Core-collapse supernovae form a hot proto-neutron star first which cools subsequently and emits a neutrino wind. That neutrino wind influences the production of heavy elements in the supernova material in the so-called r-process nucleosynthesis (see e.g. [53] and references therein). Neutron stars can collide with a corresponding emission of gravitational waves, which will be measured by gravitational wave detectors in the near future, and gamma-rays, being considered a prime candidate for gamma-ray bursts and another site for r-process nucleosynthesis. The dynamics of the collision depends on the underlying EoS of neutron stars [54]! In the future, the Square Kilometre Array (SKA) will measure more than 10 000 pulsars, with an expected 100 binary systems with a neutron star [55], so the prospects are bright for learning more about the physics of neutron stars!

References

[1] Silbar R R and Reddy S 2004 *Am. J. Phys.* **72** 892 (*Preprint* nucl-th/0309041)
[2] Shapiro S L and Teukolsky S A 1983 *Black Holes, White Dwarfs, and Neutron Stars: The Physics of Compact Objects* (New York: Wiley)
[3] Herrera L and Barreto W 2004 *Gen. Rel. Grav.* **36** 127 (*Preprint* gr-qc/0309052)
[4] Chandrasekhar S 1931 *Astrophys. J.* **74** 81
[5] Weinberg S 1972 *Gravitation and Cosmology: Principles and Applications of the General Theory of Relativity* (New York: Wiley)
[6] Landau L D 1932 *Phys. Z. Sowjetunion* **1** 285
[7] Jackson C B, Taruna J, Pouliot S L, Ellison B W, Lee D D and Piekarewicz J 2005 *Eur. J. Phys.* **26** 695
[8] Eidelman S *et al* 2004 *Phys. Lett.* B **592** 1 (http://pdg.lbl.gov)
[9] Weber F 1999 *Pulsars as Astrophysical Laboratories for Nuclear and Particle Physics* (Bristol: Institute of Physics Publishing)
[10] Hanauske M 2004 *PhD Thesis* Goethe Universität, Frankfurt am Main, Germany (http://www.th.physik.uni-frankfurt.de/~hanauske/diss_hanauske.pdf)
[11] Herrera L and Santos N O 1997 *Phys. Rep.* **286** 53
[12] Harrison B K 1965 *Phys. Rev.* **137** 1644
[13] Harrison B K, Thorne K S, Wakano M and Wheeler J A 1965 *Gravitation Theory and Gravitational Collapse* (Chicago, IL: University of Chicago Press)
[14] Glendenning N K 2000 *Compact Stars—Nuclear Physics, Particle Physics, and General Relativity* 2nd edn (New York: Springer)
[15] Gerlach U H 1968 *Phys. Rev.* **172** 1325
[16] Glendenning N K and Kettner C 2000 *Astron. Astrophys.* **353** L9 (*Preprint* astro-ph/9807155)
[17] Schertler K, Greiner C, Schaffner-Bielich J and Thoma M H 2000 *Nucl. Phys.* A **677** 463 (*Preprint* astro-ph/0001467)

[18] Oppenheimer J R and Volkoff G M 1939 *Phys. Rev.* **55** 374
[19] Haensel P, Zdunik J L and Douchin F 2002 *Astron. Astrophys.* **385** 301
[20] Prakash M, Ainsworth T L and Lattimer J M 1988 *Phys. Rev. Lett.* **61** 2518
[21] Baym G, Pethick C and Sutherland P 1971 *Astrophys. J.* **170** 299
[22] Haensel P 2001 *Physics of Neutron Star Interiors (Lecture Notes in Physics* vol 578*)* ed D Blaschke, N K Glendenning and A Sedrakian (Heidelberg: Springer) pp 127–74
[23] Ring P and Schuck P 2004 *The Nuclear Many-Body Problem* (Berlin: Springer)
[24] Akmal A, Pandharipande V R and Ravenhall D G 1998 *Phys. Rev.* C **58** 1804
[25] Lattimer J M and Prakash M 2004 *Science* **304** 536
[26] Drake J J *et al* 2002 *Astrophys. J.* **572** 996
[27] Burwitz V, Haberl F, Neuhäuser R, Predehl P, Trümper J and Zavlin V E 2003 *Astron. Astrophys.* **399** 1109 (*Preprint* astro-ph/0211536)
[28] De Luca A, Caraveo P A, Mereghetti S, Negroni M and Bignami G F 2005 *Astrophys. J.* **623** 1051
[29] Schaffner-Bielich J 2004 *Structure and Dynamics of Elementary Matter (Nato Science Series II* vol 166*)* ed W Greiner, M G Itkis, J Reinhardt and M C Güclü (Dordrecht: Kluwer) p 303 (*Preprint* astro-ph/0402597)
[30] Li G-Q, Lee C H and Brown G E 1997 *Nucl. Phys.* A **625** 372 (*Preprint* nucl-th/9706057)
[31] Weber F 2005 *Prog. Part. Nucl. Phys.* **54** 193 (*Preprint* astro-ph/0407155)
[32] Schaffner-Bielich J 2005 *J. Phys. G: Nucl. Part. Phys.* **31** S651 (*Preprint* astro-ph/0412215)
[33] Haensel P and Prószyński M 1980 *Phys. Lett.* B **96** 233
[34] Kämpfer B 1981 *J. Phys. A: Math. Gen.* **14** L471
[35] Schaffner-Bielich J, Hanauske M, Stöcker H and Greiner W 2002 *Phys. Rev. Lett.* **89** 171101 (*Preprint* astro-ph/0005490)
[36] Fraga E S, Pisarski R D and Schaffner-Bielich J 2001 *Phys. Rev.* D **63** 121702 (*Preprint* hep-ph/0101143)
[37] Macher J and Schaffner-Bielich J 2005 *Eur. J. Phys.* **26** 341 (*Preprint* astro-ph/0411295)
[38] Rajagopal K and Wilczek F 2001 *Festschrift in honor of B L Ioffe, At the Frontier of Particle Physics: Handbook of QCD* ed M Shifman (Washington, DC: National Academies Press) ch 35 p 2061
[39] Alford M 2004 *Prog. Theor. Phys. Suppl.* **153** 1 (*Preprint* nucl-th/0312007)
[40] Rischke D H 2004 *Prog. Part. Nucl. Phys.* **52** 197
[41] Alford M and Reddy S 2003 *Phys. Rev.* D **67** 074024 (*Preprint* nucl-th/0211046)
[42] Lugones G and Horvath J E 2003 *Astron. Astrophys.* **403** 173 (*Preprint* astro-ph/0211638)
[43] Baldo M, Buballa M, Burgio F, Neumann F, Oertel M and Schulze H J 2003 *Phys. Lett.* B **562** 153 (*Preprint* nucl-th/0212096)
[44] Banik S and Bandyopadhyay D 2003 *Phys. Rev.* D **67** 123003 (*Preprint* astro-ph/0212340)
[45] Blaschke D, Grigorian H, Aguilera D N, Yasui S and Toki H 2003 *AIP Conf. Proc.* **660** 209 (*Preprint* hep-ph/0301087)
[46] Shovkovy I, Hanauske M and Huang M 2003 *Phys. Rev.* D **67** 103004 (*Preprint* hep-ph/0303027)
[47] Grigorian H, Blaschke D and Aguilera D N 2004 *Phys. Rev.* C **69** 065802 (*Preprint* astro-ph/0303518)
[48] Rüster S B and Rischke D H 2004 *Phys. Rev.* D **69** 045011 (*Preprint* nucl-th/0309022)
[49] Buballa M, Neumann F, Oertel M and Shovkovy I 2004 *Phys. Lett.* B **595** 36 (*Preprint* nucl-th/0312078)
[50] Drago A, Lavagno A and Pagliara G 2004 *Phys. Rev.* D **69** 057505
[51] Alford M, Braby M, Paris M and Reddy S 2005 *Astrophys. J.* **629** 969 (*Preprint* nucl-th/0411016)
[52] Cottam J, Paerels F and Mendez M 2002 *Nature* **420** 51 (*Preprint* astro-ph/0211126)
[53] Langanke K and Martinez-Pinedo G 2003 *Rev. Mod. Phys.* **75** 819 (*Preprint* nucl-th/0203071)
[54] Oechslin R, Uryū K, Poghosyan G and Thielemann F K 2004 *Mon. Not. R. Astron. Soc.* **349** 1469
[55] Kramer M 2003 *Preprint* astro-ph/0306456